12-2018

The relationship between feeding type and temporomandibular joint morphology in superfamily Musteloidea

Travis L. Garvin
Grand Valley State University

The relationship between feeding type and temporomandibular joint morphology in superfamily Musteloidea

Travis Lee Garvin

A Thesis Submitted to the Graduate Faculty of

GRAND VALLEY STATE UNIVERSITY

In

Partial Fulfillment of the Requirements

For the Degree of

Master of Health Science

Biomedical Sciences

December 2018

Acknowledgements

I am grateful to the many people that have helped with this study. A special thanks to Laura Abraczinkas, Collections Manger, Vertebrate Collections of Michigan State University, Cody Thompson, Mammal Collections Manager of the University of Michigan, Dr. Joe Jacquot of Grand Valley State University for allowing access to their respective collections. I'd also like to thank Dr. Justin Adams of Monash University for use of the *Sarcophilus harrisii* specimens. Lastly and most important to my mentoring team of Dr. Claire Terhune of University of Arkansas, Dr. Laura Stroik of Grand Valley State University, and most importantly Dr. Melissa Tallman of Grand Valley State University for guidance in my Master's thesis study.

Abstract

Many studies have focused on the soft tissue analysis of carnivores and have demonstrated a relationship between feeding biomechanics and feeding types. Herbivores and omnivores rely heavily on anteroposterior and helical movement of the mandible and teeth for the breakdown of fibrous foods resulting in a flat mandibular fossa while the function of the carnivore TMJ is different, as they need a much stable joint for ripping and tearing of the flesh of other animals. I aim to look at whether the bony morphology of the temporomandibular joint (TMJ) morphology can be directly related to feeding type, specifically in the superfamily Musteloidea. I sampled the complete TMJ of *Gulo gulo, Lontra canadensis, Potos flavus,* and *Procyon lotor*, a dietarily diverse selection of musteloid carnivorans. I used three-dimensional scans of specimens and evaluated them by use of principal component analysis (PCA) and phylogenetic principal component analysis (pPCA) to look for data that correlated feeding type and TMJ morphology. The resulting PCA and pPCA data indicates that the feeding type is only one influential piece of bony TMJ morphology and other characteristics including locomotor habitat, soft tissue dependencies, and other non-TMJ bony characteristics contribute to the masticatory apparatus and feeding biomechanics of the TMJ. Specifically, characteristics such as snout length, coronoid process angulation, tubercle positionings, and fossa shapes, sizes, and orientations all influence TMJ morphology, and no one trait can be pinpointed as a defining characteristic for feeding type.

Table of Contents

List of Tables

Table of Figures

Introduction

Superfamily Musteloidea is a highly diverse taxonomic group comprised of over 82 species (Dumont *et al.*, 2016). The most obvious diverse aspects of this superfamily can be seen in habitat, size, and diet. Musteloids have habitats ranging from arboreal to aquatic (Dumont *et al.*, 2016), possess body sizes that span three orders of magnitude with little to no change in limb posture (Dumont *et al.*, 2016; Fabre *et al.*, 2013; Van Valkenburgh, 2007), and have highly diverse diets ranging from strict herbivory to strict carnivory. Because of the diverse nature of this superfamily, it makes for a desirable group to use in comparative anatomical studies and despite the multitude of studies on this group (Davis 2014; Dumont *et al.*, 2016; Ercoli *et al.*, 2014; Fabre *et al.*, 2013; Fabre *et al.*, 2014), there are not any studies focused on the bony aspects of the temporomandibular joint (TMJ) in addition to other characteristics of feeding. The purpose of this study is to determine if there is a relationship between diet, TMJ, morphology in musteloids. The aim is to determine if these species fill opportunistic roles within their respective environments. For example, may there have been an abundance of fruit and plant material available or perhaps there was a lack of a natural apex predator in the localized environment? In these hypothetical opportunities, it is suggested that TMJ morphology evolved to accommodate diet and fill these niches within their localized environment. Specifically, this study will examine if food types are associated with TMJ morphology in a selection of musteloids, the superfamily that consists of families Ailuridae, Mustelidae, Procyonidae, and Mephitidae. It is predicted that when there is a large percentage of meat in the diet of a musteloid, the mandibular fossa will have a more concave shape, a curvature matching convex mandibular condyle, shallower masseteric fossa, and increased in-lever out-lever distance.

Dietary diversity in carnivorans

Carnivora is the third most speciose order of mammals, consisting of more than 270 extant species; the superfamily Musteloidea encompasses nearly a third of them, with over 82 species (Dumont *et al.*, 2016; Goswami, 2006; Van Valkenburgh, 2007; Wroe and Milne, 2007). The order Carnivora is the most long-lived and successful mammalian taxon in terms of dietary divergence from an ancestral hypercarnivorous (consisting of more than 70% flesh) diet when compared to the other two mammalian orders that also exhibit carnivorous dietary adaptations (extant order Dasyuromorphia and extinct order Creodonta) (Asahara *et al.*, 2016). In fact, based on molar morphology, Asahara *et al.* (2016) concluded that dietary adaptations occurred more easily and rapidly in the evolution of order Carnivora than in the orders Dasyuromorphia and Creodonta, and therefore carnivorans may have a greater adaptive advantage over other carnivorous mammals.

Musteloids have highly diverse diets ranging from strictly herbivorous species, such as the red panda, to strictly carnivorous species, such as the wolverine. As diets vary, so do associated features. For example, species exhibit a positional gradient for the attachment point of the temporalis muscle. Herbivorous species display a temporal line lower on the neurocranium than omnivorous species, which display the temporal line closer to the midline of the cranium. Carnivorous species display a sagittal crest on the midline of the cranium (Dumont *et al.*, 2016). These differences can be attributed to the size of the temporalis muscle, a muscle that is important to generating bite force. Dumont *et al.* (2016) concluded that diet significantly influences the shape of the skull of musteloids, although not as significantly as locomotor habitat. Diet influences cranial shape because of the action of mastication, which affects the forces and sizes of associated muscles (Dumont *et al.*, 2016). However, locomotor habits may

influence braincase shape, head posture, and the shape of the orbits, whereas diet mostly affects the regions of the skull that are related to the biomechanics of biting and chewing (the snout, palate and tooth row length, the zygomatic arches, temporal line/sagittal crest). As locomotor environment is highly associated with foraging and feeding, this can lead to selective pressures that drive the skull shape in parallel directions (Dumont *et al.*, 2016). The TMJ is excluded from the discussion of the biomechanics of biting in Dumont *et al.*'s (2016) study; thus, the current study will fill that gap in our knowledge.

Anatomy of the TMJ

The skull has many complex functions, including protecting the brain, housing principal sensory organs, playing a role in food gathering and processing, drinking, vocalization, and breathing (Dumont *et al.*, 2016). The TMJ, can play a role in many of these functions and is of interest. The mammalian TMJ is a complex synovial joint formed by the condylar head of the mandible and the mandibular fossa of the temporal bone. Between these fibrocartilage-lined bony features is an articular disc, a structurally unique feature of a synovial joint (Wang *et al.*, 2011).

Synovial joints are typically comprised of hyaline cartilage, a primary cartilage of collagen type II that precedes bone formation (Wang *et al.*, 2009). A defining feature of the TMJ is the presence of fibrocartilage rather than strictly hyaline cartilage like most other synovial joints (Hylander, 2006). In other synovial joints, chondrocytes form the hyaline cartilage, and the hyaline cartilage is separated into four zones: superficial, middle, deep, and calcified (Wang *et al.*, 2009). Temporomandibular cartilage differs by having a thin proliferative zone that separates the fibrocartilaginous zones from the hyaline-like mature and hypertrophic zones. The temporomandibular condylar cartilage is composed predominately of fibroblasts and collagen

type I in the superficial fibrous zones; the underlying mature and hypertrophic zones are a mixture of both collagen types I and II, formed by differentiated fibroblasts. Therefore, the temporomandibular condyle falls under the description of fibrocartilage because of the strong presence of both type I and type II collagens, whereas hyaline cartilage contains only type II in all zones (Wang *et al.*, 2009).

Surrounding the mandibular condylar head, articular disc, and mandibular fossa is the joint capsule. This joint capsule is strengthened laterally by the temporomandibular ligament. The temporomandibular ligament is considered the major ligament of the joint, and the stylomandibular and sphenomandibular ligaments are considered minor ligaments. The stylomandibular ligament runs from the styloid process to the mandible's angle and posterior border and is lax when the jaw is closed (Alomar *et al.*, 2007; Hylander, 2006). The stylomandibular ligament only becomes tense in protrusive movement, a movement that would not be expected in normal function of carnivoran jaw movement. The sphenomandibular ligament runs from the angular spine of the sphenoid bone to the lingula of the mandible and is passive during jaw movements, keeping relatively steady tension during jaw opening and closing, although it ultimately has no influence on mandibular movements. (Alomar *et al.*, 2007; Hylander, 2006). Although this is the general morphology of the TMJ among mammals, there are exceptions to this design such as (1) the loss of the synovial cavity in some baleen whales; (2) the loss (or primitive absence) of the disc in monotremes, some marsupials, and some xenarthrans (anteaters and sloths); (3) variations of the orientation of the joint cavity from parasagittal (many rodents) to transverse (many carnivores); and (4) reversal of the convex/concave relationship so that the mandibular condyle becomes the female element as seen in many species in the order Artiodactyla (Herring, 2003).

The major muscles in charge of moving the joint are known collectively as the muscles of mastication and are split into abductors (jaw openers) and adductors (jaw closers) (Alomar *et al.*, 2007; Cox, 2008; Davis 2014). Included in the abductors are the lateral pterygoid muscles; the adductors include the masseter, temporalis, and medial pterygoid muscles (Alomar *et al.*, 2007; Bramble, 1978; Cox, 2008; Davis, 2014; Druzinsky *et al.*, 2011). Both the lateral and medial pterygoids originate from the lateral pterygoid plate of the sphenoid; the lateral pterygoid attaches at the condyle, while the medial pterygoid attaches at the bottom of the ascending ramus to the posterior edge of the angular process (Alomar *et al.*, 2007; Christiansen & Adolfssen, 2005; Cox, 2008; Davis, 2014).

The temporalis, a jaw abductor, attachment point differs based on the diet. As discussed earlier, where the herbivores display a temporal line low on the brain case, omnivorous species have a temporalis attachment close to the midline of the skull, and carnivorous species display a sagittal crest along the midline of the skull (Dumont *et al.*, 2016). The raised sagittal crest in carnivores allow for greater surface area for attachment of the temporalis. (Dumont *et al.*, 2016). The inferior attachment of temporalis is the coronoid process of the mandible. The last adductor is the masseter. The masseter has two heads: the superficial and deep head. The deep head arises from the ventral part of the zygomatic arch and inserts on the lateral border of the ramus. The superficial head originates on the zygomatic process of the maxilla and inserts on the mandibular ramus (Christiansen and Adolfssen, 2005; Hylander 2006).

Two other muscles of interest are the mylohyoid and digastric muscles. The mylohyoid is situated under the jaw attaching at the lower anterior surface of the hyoid bone and the mylohyoid line of the mandible (van Eijden and Koolstra, 1998). In addition to being the diaphragm of the mouth, the mylohyoid aids in respiration, deglutition, and phonation (Yamaoka

et al., 1992). The mustelid digastric muscle arises from the jugular process of the occipital bone and a variable portion of the juglomastoid ridge and inserts on the medial and lateral sides of the mandible around the first and second mandibular molars (M_1 and M_2). Between the two attachment points, the digastric muscle is divided into two muscle bellies by a common tendon. The digastric muscle of carnivores is large relative to other animals and functions as a jaw abductor (Scapino, 1976). It is believed that the function of the digastric in carnivores is to help aid the opening of the jaw widely and rapidly immediately prior to the apprehension of prey, as well as disengaging the canines from flesh and bone of the intact prey (Scapino, 1976).

Anatomy and feeding biomechanics in carnivorans

It has been shown that mastication and the associated muscles have a direct effect on cranial shape (Dumont *et al.*, 2016). Figueirido (2010) found that skull shape not only correlates with feeding behavior but also with phylogenetic relatedness. Because all herbivorous carnivorans evolved from generalized carnivorans (Van Valkenburgh, 2007), adaptations to the carnivoran skull towards herbivory have been interpreted as functional traits and allow for high bite forces similar to hypercarnivorous species (Christiansen and Wroe, 2007). The potential for high bite forces in herbivorous carnivoran species is constrained by functional solutions dictated by natural selection within the possibilities allowed by extrinsic factors (natural selection) as well as intrinsic ones (shared developmental pathway) (Figueirido, *et al.*, 2010). Some limitations include fixed TMJs and tooth occlusion where together teeth are prevented from grinding foods. Coupling a short digestive tract without a caecum, digestive microbiota with a low digestibility rate of cellulose and carbohydrates, and the inability to grind food, herbivorous carnivorans must eat large quantities of food, encouraging large muscle development of the masseter and temporalis. Because of the well-developed masseter and temporalis, it allows for

the capacity for high bite forces like that those of carnivorous mammals (Figueirido, *et al.*, 2010). Despite herbivorous carnivorans generating similar bite forces as carnivorous non-carnivoran mammals (Figueirido *et al.*, 2010), they rely more on relatively larger masseter muscles rather than a well-developed temporalis (with the exception of *Ailurus fulgens*, the red panda) (Bramble, 1978; Dumont *et al.*, 2016). The dependence on these muscles can also explain differences in cranial morphology among feeding types. For example, compared to other feeding types, herbivores are expected to have a larger zygomatic arch, the point of the origin for the masseter, as the masseter is biomechanically advantageous for higher bite forces at low gape (Dumont *et al.*, 2016). Just as an herbivore is more dependent on the masseter, the carnivores are more dependent on the temporalis, which attaches at a raised sagittal crest, allowing for the generation of a higher bite force at high gapes (Turnbull, 1970). Lastly, both herbivorous and carnivorous species have a shorter snout than omnivores. The shortest snout is seen in carnivorous mustelids, as they need to generate high bite forces at the canines (Dumont *et al.*, 2016). This is of importance as maximum bite force is an important metric of feeding performance that defines the feeding ecology of many vertebrates (Santana, 2016).

The cranium and jaw are crucial to the capture, killing, and processing of prey, and the masticatory muscles are activated to allow the opening and closing of the jaw as well as generating bite forces (Dumont *et al.*, 2016). A crucial metric of bite force is jaw gape. It is hypothesized that one hundred percent of jaw gape seen in carnivores is achieved through condylar rotation, as the center of rotation passes through the mandibular condyle (Terhune *et al.*, 2011). This relates to the morphology of the TMJ because the preglenoid and postglenoid processes restrict the movement of translational movement of the mandible. Shallower gapes of carnivores produce higher bite forces at both the canines and the carnassials, though optimal

gape is observed between 25 and 35 degrees in the carnivoran *Canis lupus dingo* (Bourke *et al*., 2008). Compare that to primates who all show translational movement in the jaw as part of the chewing cycle (Terhune *et al*., 2011). Specifically, *Cebus apella* exhibits a jaw movement similar to humans, where approximately 23% of jaw gape in humans is attributed to condylar translational movement (Terhune *et al*., 2011).

Like *Cebus apella*, herbivores and omnivores rely heavily on: (1) anteroposterior translation of the mandible in jaw opening; and (2) helical movement of the TMJ, making it possible for the grinding and breakdown of the fibrous foods they consume. Because of the increased range of motion, the morphology of the joint is a very flat mandibular fossa with indistinct preglenoid and postglenoid processes. Specifically, when comparing carnivores to non-carnivores, the shape of the carnivore postglenoid and preglenoid processes are enlarged and encircled around the head of the mandibular condyle, restricting translational movement of the joint (Noble, 1973). The joint capsule further restricts excessive protrusive and retrusive movements of the condyle in mammals, though mediolateral translation occurs (Hylander, 2006). The increased stability of the joint is attributed to the need to capture and subdue prey, ultimately reducing the risk of dislocating the TMJ during feeding (Maynard-Smith and Savage, 1959).

This study will compare the TMJ and associated masticatory features within the superfamily Musteloidea in the strict meat-eaters, omnivores, and frugivores and will determine whether food type is associated with the increased stability of the joint. Overall, the expected pattern is that the larger percentage of meat in the diet of a musteloid, the mandibular fossa will have a more concave shape, a curvature matching convex mandibular condyle, shallower masseteric fossa, and increased in-lever out-lever distance. Conversely, musteloids consuming more fruit and plant material in their diet will exhibit a less concave mandibular fossa and less

convex mandibular condyle, deeper masseteric fossa, and decreased in-lever out-lever distance. Omnivores are expected to be in the middle of these, with a slight concave curvature of the mandibular fossa and a slight convex curvature to the mandibular condyle and a medium depth masseteric fossa, and middle in-lever out-lever distance. These expectations were developed by following the logic found in Table 2. The general idea is that restricted joint morphology of the carnivore TMJ is a result of the constraints on feeding. The same logic can be said for the opposite end of the feeding spectrum where the lack of physical constraints on feeding result in a less restricted joint morphology in more herbivorous taxa.

Table 1. Chart of predictions based on generalized characteristics of each feeding type in musteloids.

Prediction Table			
	Carnivore	Herbivore/Frugivore	Omnivore
Mandibular Condyle/Mandibular Fossa	Mandibular condyle will have a convex shape	Mandibular condyle will have a flatter, less convex shape	Mandibular condyle and Mandibular fossa curvature will fall between the Carnivore and Herbivore
Muscle dependency-Masseteric fossa characteristic	Reliance on temporalis, smaller masseteric fossa	Reliance on masseter, larger masseteric fossa	Semi-dependent on both masseter and temporalis, medium masseteric fossa
In-lever/Out-lever distance	In-lever distance large relative to out-lever	In-lever distance small relative to out-lever	In-lever distance medium relative to out-lever

Table 2. Chart of assumptions based on generalized characteristics of each feeding type in musteloids.

Morphological Assumptions Based on Feeding Types			
Assumption	Carnivore	Herbivore/Frugivore	Omnivore
Defining Feeding Types	Animals that eat other animals >70% of diet (e.g., carnivore, piscivore, insectivore)	Animals that eat plant matter >70% of diet (e.g., frugivore, herbivore, folivore)	Animals that eat >30% plant matter and >30% animals
Food Locomotion and Defense	Prey moves and has ability to escape consumption by predator/has a defense system against consumption (e.g., mollusks)	Food consumption does not involve predation and food product does not have a chance of escaping after capture	Mixture of both food consumption in which food either has or lacks ability to move
Constraints on Feeding	Greater chance of jaw displacement due to prey movement and ripping and tearing of flesh	Low chance of jaw displacement based on food consumption. Chewing and grinding fibrous foods is the primary form of consumption	Some chance of jaw displacement based on food consumption
Reaction to Constraints	Great stability of the TMJ	Little stability of the TMJ	Moderate stability of the TMJ
Morphology Description	More cylindrical/concave mandibular fossa and more cylindrical/convex mandibular condyle	Flatter mandibular fossa and flatter mandibular condyle	Moderate cylindrical/concave mandibular fossa and moderate cylindrical/convex mandibular condyle

Materials and Methods

The study included the crania of 86 specimens and mandibles of 73 specimens across six different species, four of which were from the superfamily Musteloidea. The species were chosen based on diet to include: strict carnivores (family Mustelidae), omnivores and strict frugivores (family Procyonidae). The strict Mustelidae carnivores included in this study are the North American river otter (*Lontra canadensis*) and the wolverine (*Gulo gulo*). Included in the study within the family Procyonidae are the omnivorous raccoon (*Procyon lotor*) and the strictly frugivorous kinkajou (*Potos flavus*).

Table 3. Data table of frequency of occurrence of food types and sex distribution amongst the six species.

Species	Sex Distribution and Frequency of occurrence (%)									
	Sex				Flowers, Leaves, and Plant material	Fruit	Vertebrates	Invertebrates	Other	Specimen Access
	M	F	U	Total						
Ateles geoffroyi[a]	8	6		14	20.9	77.7		1.3		Grand Valley State University
Gulo gulo[b]	*10*	*2*	*1*	*13*			100			Michigan State University, University of Michigan
Lontra canadensis[c]			*16*	*16*			61.2	38.8		Grand Valley State University
Potos flavus[d]	9	7		16	9.3	90.7				Michigan State University
Procyon lotor[e]	8	6		14	19.9	13.2	10.3	50.3	6.6	Grand Valley State University
Sarcophilus harrisii[f]			13	13			97.0	3.0		Monash University

[a]Chapman (1987); [b]Inman (2015); [c]McMillan *et al.* (2015); [d]Rulison *et al.* (2012); [e]Kays (1999); [f] Pemberton *et al.* (2012).

In addition to the variable dietary profiles (Table 3), taxa within the Musteloidea span three orders of magnitude in size, but these four species are relatively similar in size to one another. Second, this group includes arboreal, terrestrial, and aquatic species. This is important because locomotor habitat plays a large role in cranial shape. By including the species within this study, I was inclusive of all locomotor habitats. It was expected that the species of superfamily Musteloidea could have some common traits as a result of their shared common ancestor (Figure

1) (dated to approximately 27.4 million years ago) (Slater *et al.*, 2012). All herbivorous carnivorans evolved from a carnivorous ancestor (Van Valkenburgh, 2007), with a body plan established in the phylogeny Carnivora. The morphological resemblance of an herbivorous musteloid skull to a carnivorous musteloid skull could be driven by extrinsic factors (e.g., natural selection) and intrinsic factors (e.g., shared developmental pathway). Intrinsic factors may impose constraints on the direction of skull shape evolution towards herbivory. (Figueirido, 2010). Because of these factors, the morphological differences in the TMJ within Musteloidea could be considered functional adaptations from diet or phylogenetic similarity resulting from divergence which this study is designed to help clarify.

A frugivorous species, Geoffroy's spider monkey (*Ateles geoffroyi*), and a carnivorous species, the Tasmanian devil (*Sarcophilus harrisii),* outside of the order Carnivora are used as controls. By including *Ateles geoffroyi* and *Sarcophilus harrisii* in the study, a control for phylogeny is introduced, as the *Ateles geoffroyi* and Musteloidea's common ancestor diverged 83.8 million years ago (Reis *et al.*, 2012), and *Sarcophilus harrisii* and Musteloidea's common ancestor diverged 160.0 million years ago (Cao *et al.*, 2000). The relatively large time in ancestral divergence between these two taxa and Musteloidea species means that any morphological similarities would be the result of convergent evolution for the same function rather than caused by phylogenetic similarity.

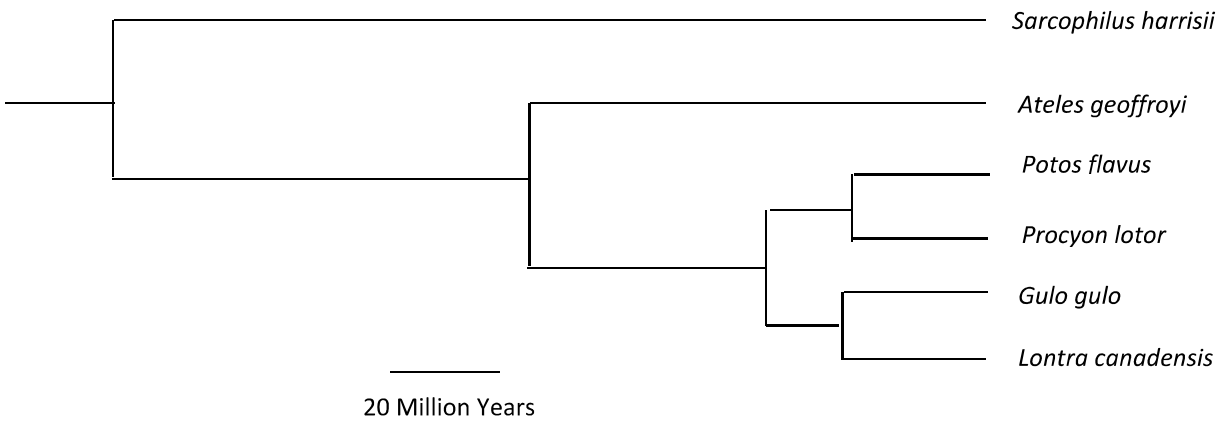

Figure 1: Phylogenetic tree for the species included in this study. *Gulo gulo* and *Lontra canadensis* diverged 26.4 Ma (Arnold *et al*., 2010). *Potos flavus* and *Procyon lotor* diverged 24.8 Ma (Arnold *et al*., 2010). Procyonidae (*Procyon lotor* and *Potos flavus*) and Musteloidea (*Gulo* and *Lontra canadensis*) diverged 39.9 Ma (Arnold *et al*., 2010). *Ateles geoffroyi* shared a common ancestor with Musteloidea species at 83.8 Ma (dos Reis, 2012). *Sarcophilus harrisii* shared a common ancestor with Musteloidea and *Ateles geoffroyi* species at 160.0 Ma (Cao *et al.*, 2000).

Data Collection

Landmark Editor (Wiley *et al*., 2005) was used for data collection. Digital models of each of the mandibles and crania used in the study were collected using three-dimensional (3D) surface scans of each specimen using a NextEngine 3D scanner. The scanner was set to the macro setting using seven slices to construct the image. I used multiple scans, typically two or three of each specimen, and they were manually aligned using Geomagic Studio 2014.

A landmark protocol consisting of single points, as well as 4X4, and 5x5 patches on both the mandible and cranium was used (Tables 3-4). A landmark is described as a discrete anatomical locus that may be biologically or mathematically homologous (Cooke and Terhune, 2015). Bookstein (1991) originally classified landmarks into three types: Type 1- discrete juxtapositions of tissues; Type 2 - maxima of curvature; and Type 3 - external points or points that are defined by virtue of information at other locations on that object. Type 3 landmarks originally included semilandmarks. Semilandmarks have been further defined as three separate types of semilandmarks: Type 4 - semilandmarks on curves; Type 5 - semilandmarks on surfaces; and Type 6 - constructed semilandmarks (Cooke and Terhune, 2015).

The single points used within the study are a combination of type 1, 2, and 3 landmarks. The landmark patches, Type 5 semilandmarks, consist of nine points (3x3) placed by the researcher. The program generates the remaining landmarks based on midpoints of the original patch points, all being equidistant from the landmarks in their respective positions. Semilandmarks were slid into their most mathematically homologous positions by minimizing the Procrustes distances among the specimens, using *geomorph*, an R package for the collection and analysis of geometric morphometric shape data (Adams and Otárola-Castillo, 2013). Sliding semilandmarks are now more commonly used than strict homology landmarks as they allow for

the identification of landmarks that may not be strictly biologically homologous but are instead mathematically homologous (Cooke and Terhune, 2015). This is to say they are computer generated landmarks rather than relying on the researcher for accurate placement on homologous landmarks.

Landmark points for the mandible were placed via the protocol in Table 4, with corresponding example images in Figure 2. Single points were placed on the alveolar margin along the tooth row, on the medial side of the mandible, and the most superior point of the coronoid process. Single points were placed for multiple reasons. First, the single points of the tooth row helped establish mandible shape most notably in relation to mandible length and angulation of the mandible. Second, they help act as anchor points to limit manipulation of the patches dorsal to the single points of the alveolar margin during analysis. The single points placed at the medial side of the mandible and coronoid process reference anchor points of pterygoid and temporalis muscles, respectively. Patches were used on the masseteric fossa and mandibular condyle. The patch of the masseteric fossa helps explain dependency of the masseter muscle during mastication. The mandibular condyle patch was included as this patch would best exemplify the shape of the joint.

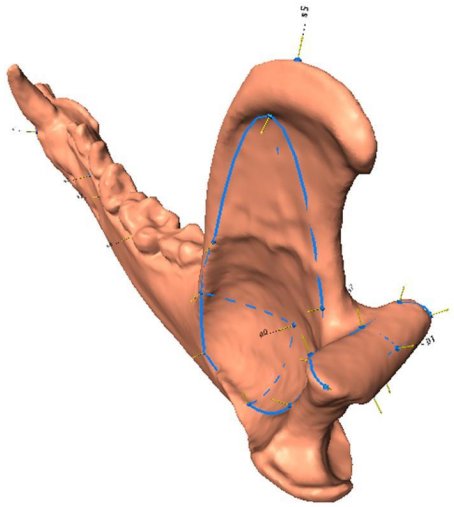

Figure 2. An example of the landmarking protocol described in Table 4 on *Procyon lotor* left mandible.

Table 4: Description of landmarking protocol of the mandible. Points are matching the Procrustes fit diagram in Figure 2.

Mandible	
Point	Description
S0	Alveolar margin, midline I1 (Anterior View)
S1	Alveolar margin, midline Canine (Lateral View)
S2	Alveolar margin, midline P3 (Lateral View)
S3	Alveolar margin, midline P4 (Lateral View)
S4	Alveolar margin, midline M1 (Lateral View)
S5	Most superior point of coronoid process
S6	Anteroinferior point of pterygoid fossa
S7	Posteroinferior point of pterygoid fossa
P1-1	Anteroinferior point of masseteric fossa
P1-2	Inferior Midpoint of masseteric fossa
P1-3	Posteroinferior point of masseteric fossa
P1-4	Anterior mid-point of masseteric fossa
P1-5	Mid-point of masseteric fossa
P1-6	Posterior mid-point of masseteric fossa
P1-7	Anterosuperior point of masseteric fossa
P1-8	Superior point of masseteric fossa
P1-9	Posterosuperior point of masseteric fossa
P2-1	Anterolateral point of mandibular condyle
P2-2	Anterior mid-point of mandibular condyle
P2-3	Anteromedial point of mandibular condyle
P2-4	Lateral mid-point of mandibular condyle
P2-5	Mid-point of mandibular condyle
P2-6	Medial mid-point of mandibular condyle
P2-7	Posterolateral point of mandibular condyle
P2-8	Posterior mid-point of mandibular condyle
P2-9	Posteromedial point of mandibular condyle

Landmark points for the cranium were placed via protocol in Table 5, with corresponding example images in Figure 3. Again, single points were placed on the alveolar margin along the tooth row, and in addition, on the most inferior point on the pterygoid plate. The single points of the tooth row helped establish the snout length of the specimen and act as an anchor point for the patch located dorsal of the alveolar margin during analysis. The single point of the pterygoid plate is included as a pterygoid muscle attachment point relating to feeding. The patch on the mandibular fossa was used to exemplify the shape of the joint surface.

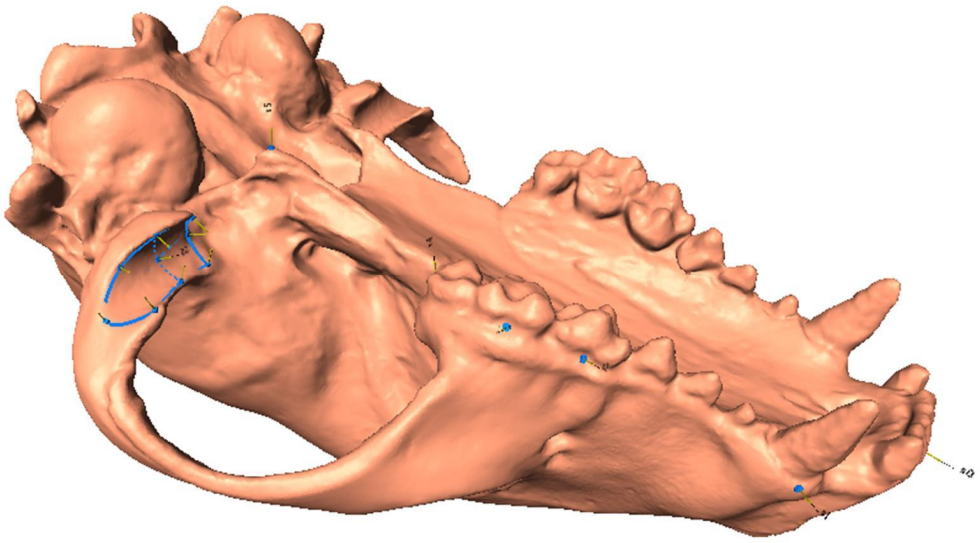

Figure 3. An example of the landmarking protocol described in Table 5 on a *Procyon lotor* cranium.

Table 5. Description of landmarking protocol of the cranium. Points match the Procrustes fit diagram in Figure 3.

Cranium	
Point	Description
S0	Alveolar margin, midline of skull (Anterior View)
S1	Alveolar margin, midline Canine (Lateral View)
S2	Alveolar margin, midline P4 (Lateral View)
S3	Alveolar margin, midline M2 (Lateral View)
S4	Maxillary Tubercle
S5	Most inferior point on pterygoid plate
P1-1	Anterolateral point of mandibular fossa
P1-2	Anterior mid-point of mandibular fossa
P1-3	Anteromedial point of mandibular fossa
P1-4	Lateral mid-point of mandibular fossa
P1-5	Mid-point of mandibular fossa
P1-6	Medial mid-point of mandibular fossa
P1-7	Posterolateral point of mandibular fossa
P1-8	Posterior mid-point of mandibular fossa
P1-9	Posteromedial point of mandibular fossa

Data Analysis

Error study

An intraobserver error study was first run to determine the legitimacy of the landmarking protocol described in the data collection section. The following description applies to both landmarking of the crania and mandibles. To perform the intraobserver study, landmarks were placed on five replicates of a *Procyon lotor* individual, as well as five different individuals of the same species. A generalized Procrustes analysis (GPA) was run comparing the samples in each respective group. A GPA superimposes all landmark configurations by minimizing the sum of squares distance among specimens. This means that after Procrustes superimposition, translation and rotation are removed as variables, and configurations are scaled to a common unit size. This allows for the shape alone to be analyzed, as shape is considered the most important element in comparative analysis. Procrustes distance is the square root of the summed squared distance between homologous landmarks in two landmark configurations after Procrustes superimposition. The larger the difference in the Procrustes distances between the trials and the mean, the more different the specimens are; thus, Procrustes distance is a good measure of intraobserver error (Adams, Rohlf, & Slice, 2004; Cooke and Terhune, 2015; Sundberg, 1989).

A t-test was then run to determine if landmark points were placed accurately and precisely. A t-test of a successful landmarking protocol shows a significant difference between the same specimen landmarks and the landmarks of a different specimen. If the t-test showed that the landmark is not a good point (no significant difference in the t-test), the landmark was not used in the analysis. Results of the mandible t-test can be seen in Table 6 and results of the cranium t-test can be seen in Table 7. Within the tables there are some points (landmarks 9, 10, 11, 30, 31, 32, in the mandible and landmarks 17 and 21 in the cranium) that do not show a

significant difference. These points, however, are still used in analyses as they were midpoints in patches, and were thus generated by the computer and were not yet slid into proper placement.

Table 6: T-test error study results of the mandible. Within the table there are some points (landmarks 9, 10, 11, 30, 31, 32) that do not show a significant difference. These points are still used within the analyses as they are midpoints generated by the computer and are not yet slid into proper placement.

Mandible Error Study Results			
Landmark Point	P-Value	Landmark Point	P-Value
1	.043	30	.055
2	.011	31	.052
3	.004	32	.052
4	.028	33	.040
5	.033	34	.011
6	.030	35	.043
7	.011	36	.039
8	.009	37	.025
9	.057	38	.013
10	.057	39	.002
11	.053	40	.020
12	.047	41	.021
13	.001	42	.014
14	.036	43	.001
15	.043	44	.008
16	.044	45	.044
17	.022	46	.048
18	.024	47	.011
19	.047	48	.004
20	.035	49	.018
21	.041	50	.039
22	.032	51	.047
23	.018	52	.028
24	.047	53	.011
25	.039	54	.033
26	.049	55	.027
27	.040	56	.030
28	.021	57	.031
29	.048	58	.037

Table 7: T-test error study results of the cranium. Within the table there are two points (landmarks 17 and 21 in the cranium) that do not show a significant difference. These points are still used within analysis as they are midpoints generated by the computer and are not yet slid into proper placement.

Cranium Error Study Results			
Landmark Point	P-Value	Landmark Point	P-Value
1	.007	12	.005
2	.016	13	.039
3	.015	14	.021
4	.006	15	.009
5	.017	16	.011
6	.004	17	.084
7	.000	18	.025
8	.027	19	.000
9	.000	20	.020
10	.000	21	.188
11	.011	22	.010

The first step of the data analysis was collecting the landmarks in Landmark Editor, following the landmark protocol described in Table 4 for the mandible and Table 5 for the cranium. After the data were collected, a GPA with sliding semilandmarks was performed in R using the *geomorph* package (Adams and Otárola-Castillo, 2013). A principal component analysis (PCA) was run on five different groupings including Musteloidea mandible and crania, Musteloidea with *Ateles geoffroyi* mandible and crania, and Musteloidea with *Ateles geoffroyi* and *Sarcophilus harrisii* cranium to explore patterns of variability among the sample. Because most landmarking configurations are not simple, the resulting shapes can be difficult to interpret and analyze. PCA is a mathematical algorithm that reduces the dimensionality of the data while retaining most of the variation of the data, making the data easier to interpret (Ringnér, 2008).

Next, the phylogeny was mapped onto the data to test whether there was a significant relationship between shape and phylogeny. If a significant portion of shape (signified by a p-value <0.05) within the data was related to phylogeny, a phylogenetically corrected PCA (pPCA) was performed. As data for species may be nonindependent due to a shared evolutionary history, phylogenetic information should not be ignored (Revell, 2009). A “normal” PCA is based on a

singular value decomposition of a covariance matrix of the Procrustes aligned data. However, a pPCA uses the phylogenetic independent contrasts as the basis of that covariance matrix and PC scores for each original specimen are calculated post hoc using the scaled eigenvectors from the pPCA. This process creates a PCA where the only shape variation present on each axis is uncorrelated with phylogeny (Revell, 2009).

The study of the relationship between size and shape is known as allometry (Cadima & Jolliffe, 1996). After the PCA analysis was finished, a regression test was also run to test how much variation in the sample was related to allometry. The regressions were performed two ways: (1) pooled by genus, which looks for a common allometric trajectory among groups; and (2) unpooled, which looks for a relationship from smallest specimen to largest specimen. A p-value <0.05 signifies a significant difference.

Results

Mandibles

A PCA of all musteloids can be seen in Figures 4 and 5, and PC information is provided in Table 8. On the first PC axis, there is a pattern to the data with a short S5 (most superior point of coronoid process) to P2-2 (anterior mid-point of mandibular condyle). PC1 (Figure 4) accounts for 43.3% of the variability in the sample and represents shape variation relating to the angulation of the coronoid process, tilt of the head of the mandibular condyle, and depth of the masseteric fossa. Individuals at the negative end of PC1 (*Potos flavus*) have a coronoid process angled posteriorly, inferiorly tilted mandibular condyle on the medial side, and shallower masseteric fossae, while individuals at the positive end of PC1 (*Lontra canadensis*) have slightly anteriorly angled coronoid processes, no tilted condyle, and deeper masseteric fossae. On the second PC axis, there is a pattern to the data with masseter-dependent species to the negative end, and temporalis-dependent species to the positive end. PC2 (Figure 4) accounts for 22.6% of the variability in the sample and represents shape variation relating width of the masseteric fossa and height of the coronoid process. Individuals at the negative end of PC2 (*Gulo gulo*) have much wider fossae and a short coronoid process. Individuals near the positive end of PC2 (*Lontra canadensis, Potos flavus, Procyon lotor*) have much narrower masseteric fossae and a tall mandible.

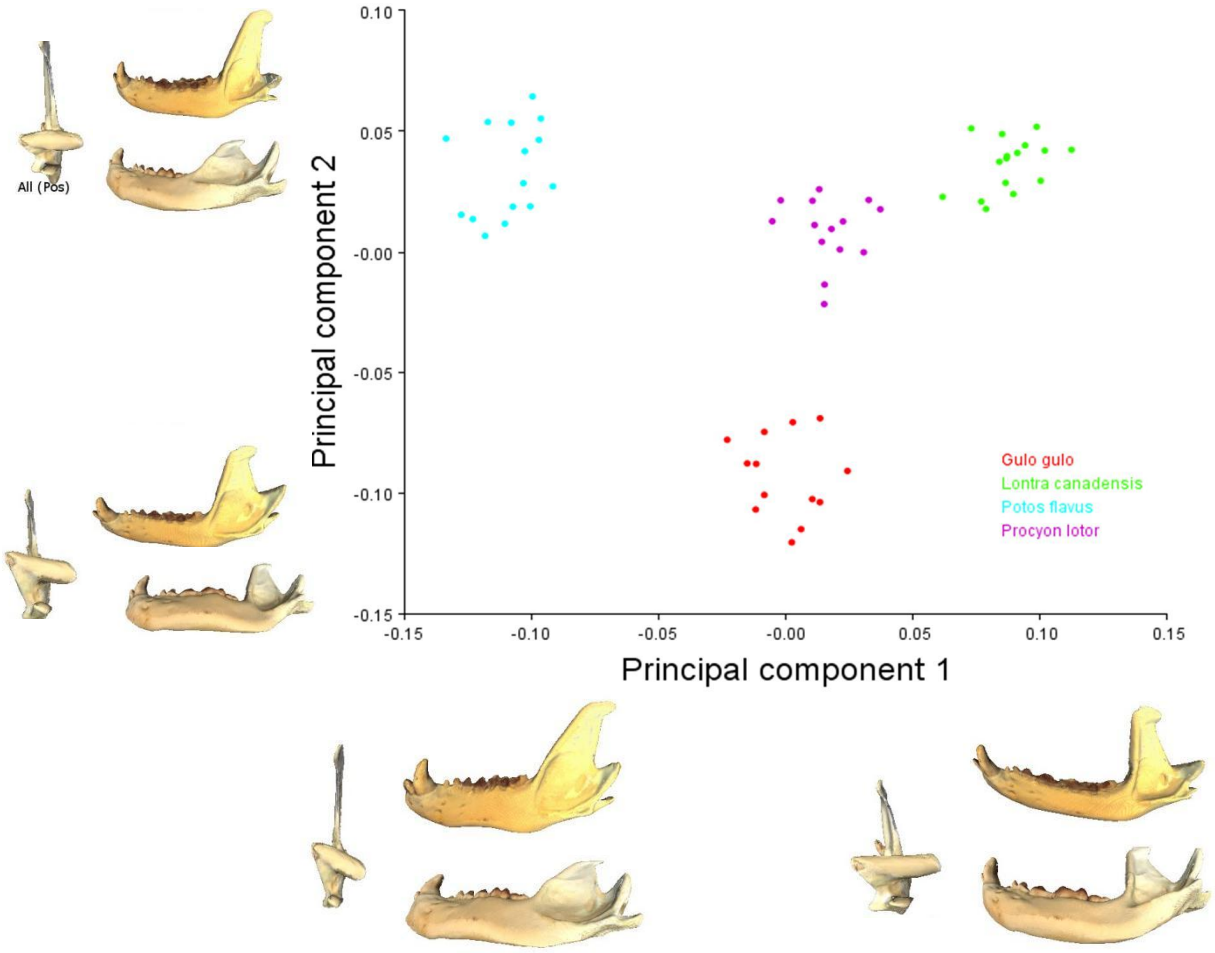

Figure 4. Results of the principal component analysis performed on Musteloidea mandibles. Each dot represents a single specimen. It is thought that species are grouped by biomechanical advantages on PC1. PC2 is grouped by muscle dependency. Mandibles are in lateral (top), latero-inferior (bottom), and caudal (left) views.

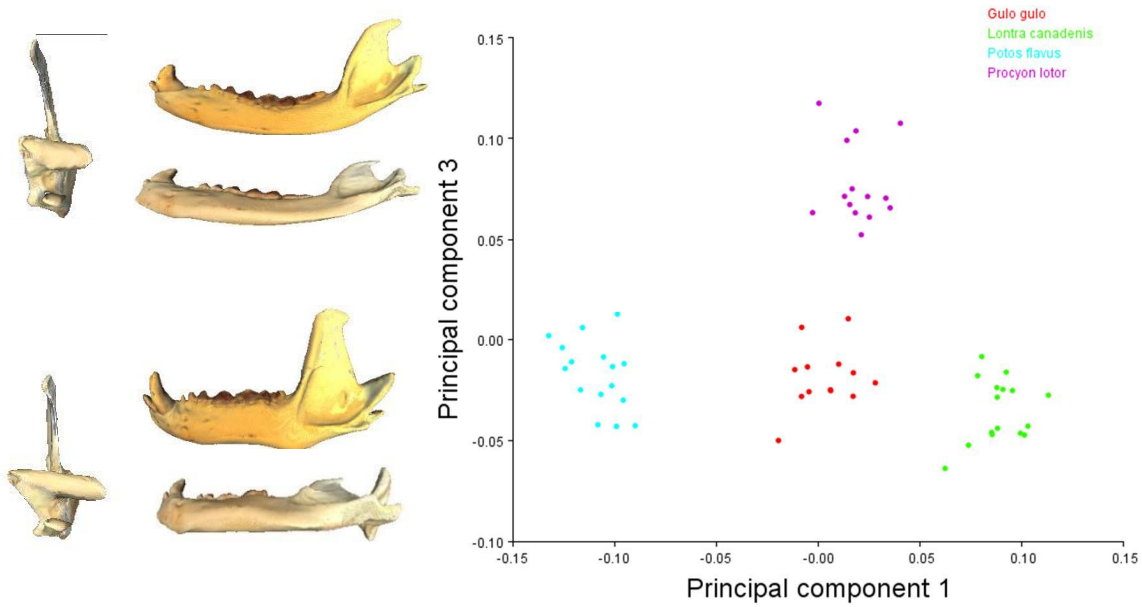

Figure 5. Results of the principal component analysis performed on Musteloidea mandibles. Each dot represents a single specimen. Species are grouped by diet on PC3. Mandibles are in lateral (top), latero-inferior (bottom), and caudal (left) views.

Lastly, on PC3, the strict herbivore and carnivores are located on the negative end, and the omnivore on the positive end. PC3 (Figure 5) accounts for 17.9% of the variation and relates to the position of the superior point of the coronoid process, mandible length, and condylar head width. Individuals at the negative end (*Gulo gulo, Lontra canadensis, Potos flavus*) have no distinct change in the most superior point of the coronoid process, shorter mandibles anterior-posteriorly, and a wide condylar head. Individuals with positive PC3 values (*Procyon lotor*) have a posteriorly positioned coronoid process and a longer mandible. There was no significant relationship between shape and phylogeny (p=0.3320) (Table 9).

Table 8. PC score variation within each graph displaying the amount of variation being concentrated within the first three PCs.

% variation on each PC axis					
	Related Figures	PC1 (%)	PC2 (%)	PC3 (%)	Total Variation (PC1-3) (%)
Mandible					
Musteloidea	4,5	43.266	22.587	17.879	83.733
Musteloidea Articular Surface	6	54.562	13.595		68.157
Musteloidea with *Ateles geoffroyi*	7,8	74.547	11.829	5.135	91.511
Musteloidea with *Ateles geoffroyi* Articular Surface	9	53.674	15.721		68.945
Cranium					
Musteloidea	10,11	46.421	26.673	12.441	87.535
Musteloidea Articular Surface	12	61.928	10.999		72.927
Musteloidea (Phylogenetically Corrected)	13,14	46.493	34.752	18.756	100.000
Musteloidea with *Ateles geoffroyi* and *Sarcophilus harrisii*	15,16	57.556	18.347	9.587	85.760
Musteloidea with *Ateles geoffroyi* and *Sarcophilus harrisii* Articular Surface	17	68.413	15.280		83.693

A PCA of the Musteloidea articular surface can be seen in Figure 6, and PC information is provided in Table 8. On the first PC axis, there is a distinct pattern to the data with strict carnivores at the negative end, and the strict herbivore to the far positive end. PC1 (Figure 6) accounts for 54.6% of the variability in the sample and represents shape variation relating to the curvature of the mandibular condyle. Individuals at the negative end of PC1 (*Lontra canadensis*) show very dramatic curvature to the mandibular condyle, while individuals at the positive end of PC1 (*Potos flavus*) still have a curved mandibular condyle, though this curvature is less pronounced and is very broad and long. On the second PC axis, there is a no distinct pattern to the configuration. PC2 (Figure 6) accounts for 13.6% of the variability in the sample and

represents shape variation relating anterior-posterior curvature of the mandibular condyle. Individuals at the negative end of PC2 (*Gulo gulo*) have a straight anterior edge. Individuals near the positive end of PC2 (*Lontra canadensis, Potos flavus, Procyon lotor*) have a slight curvature, or bowing, with the middle of the condyle more posteriorly positioned. While the overall differences in positive PC2 and negative PC2 are present, the differences are much less dramatic and noticeable than that of PC1.

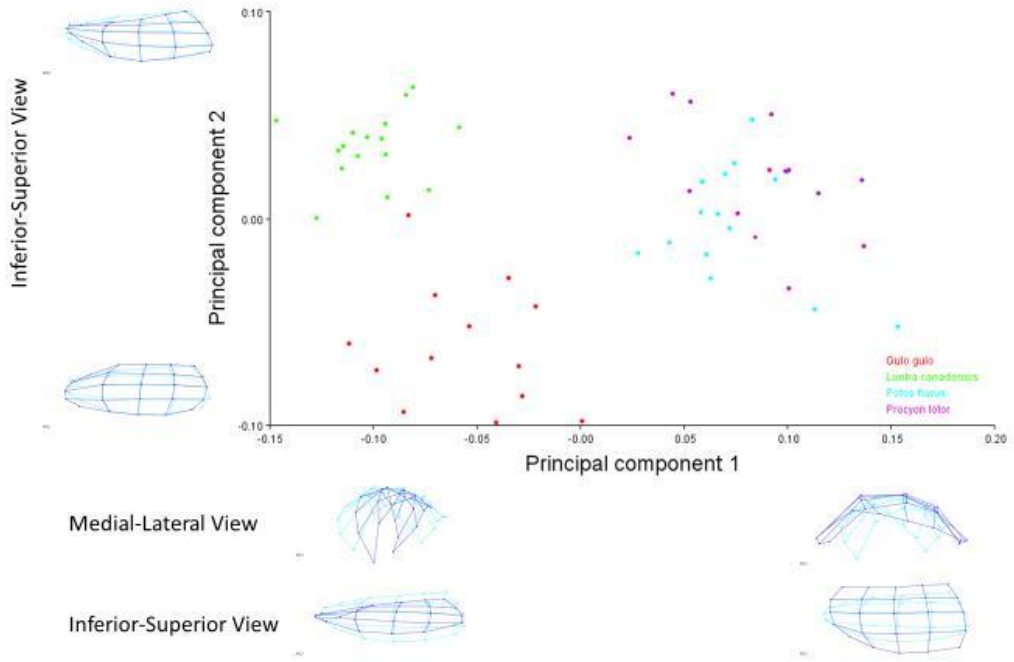

Figure 6. Results of the principal component analysis performed on Musteloidea mandibular condyle. Each dot represents a single specimen. Species are grouped by diet on PC1. On PC1 axis, the mandibular condyles are in medial-lateral view (top), inferior-superior view (bottom). There is no distinct patterning on PC2. The light blue represents the average with the PC change overlaid in a purple.

PCAs of musteloids with *Ateles* can be seen in Figures 7-8 and Table 8. On the PC1 axis, non-Musteloidea herbivores are on the positive end, and carnivorans are on the far negative end. However, herbivorous Musteloidea are pulled in the direction of the positive end of PC1, indicating greater similarity to the non-Musteloidea herbivores than the carnivorous Musteloidea

to the non-Musteloidea herbivores. The placement of the carnivorous *Lontra canadensis* in relation to the omnivorous *Procyon lotor* can be explained by the dependency on the masseter. This is consistent with results in Figure 4, where the dependency on the masseter is the driving factor. PC1 (Figure 7) accounts for 74.5% of the variability in the sample and represents shape variation related to the width and shape of the masseteric fossae and the positioning of the mandibular condyle. Individuals at the negative end of PC1 (*Gulo gulo)* have a very narrow masseteric fossa. The mandibular condyle is inferior on the mandible with the articulating surface in a superior-inferior orientation. Individuals at the positive end of PC1 (*Ateles geoffroyi*) have a very broad masseteric fossa, and the mandibular condyle is superior on the mandible with the articulating surface in an anterior-posterior orientation. There is no distinct patterning within PC2, with herbivores, omnivores, and carnivores dispersed throughout the data sample. PC2 (Figure 7) accounts for 11.8% of the variation in the sample and represents coronoid process angulation and characteristics of the condyle. Individuals at the negative end of the spectrum (*Potos flavus*) have shallow masseteric fossae, and the superior point of the coronoid process is positioned posteriorly. The mandibular condyle is also tilted inferiorly on the medial side and is narrow. Individuals at the positive end of the spectrum (*Lontra canadensis*) have deep masseteric fossae, and the superior point of the coronoid process is positioned anteriorly. The mandibular condyle shows no tilt and is very wide. Like PC2 musteloid mandible group, PC3 in the musteloids with *Ateles* grouping is patterned based on diet. Carnivores and herbivores group tightly together on the negative end, and omnivores are the outlying group on the positive end. PC3 (Figure 8) accounts for 5.1% of the variation and represents differences in condyle width and mandible length. Individuals at the positive end of PC3 (*Procyon lotor*) have a very narrow condylar head and a longer mandible in length. Individuals at the negative end of PC3 (all other

taxa) have an extremely wide condylar head and a short mandible. Shape was not significantly correlated with phylogeny with a p-value of 0.68 (Table 9).

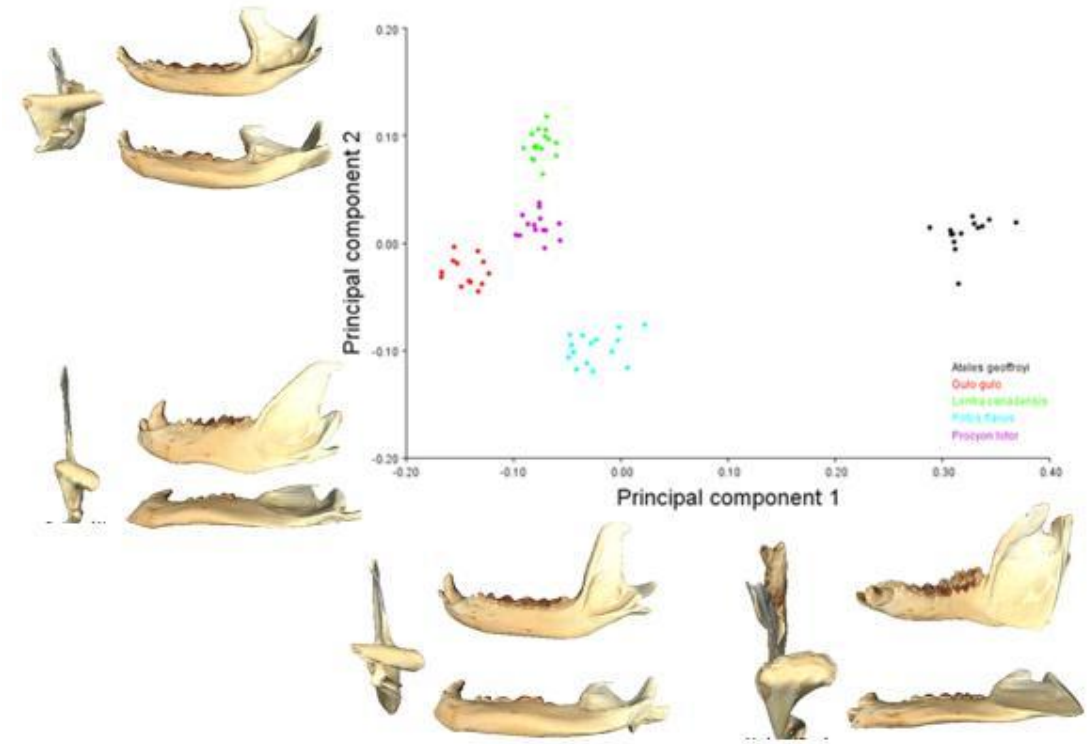

Figure 7. Results of the principal component analysis performed on Musteloidea with *Ateles geoffroyi* mandibles. Each dot represents a single specimen. Species are grouped by muscle dependency on PC1, and mechanical advantage of temporalis on PC2. Mandible views include lateral, latero-inferior, and caudal

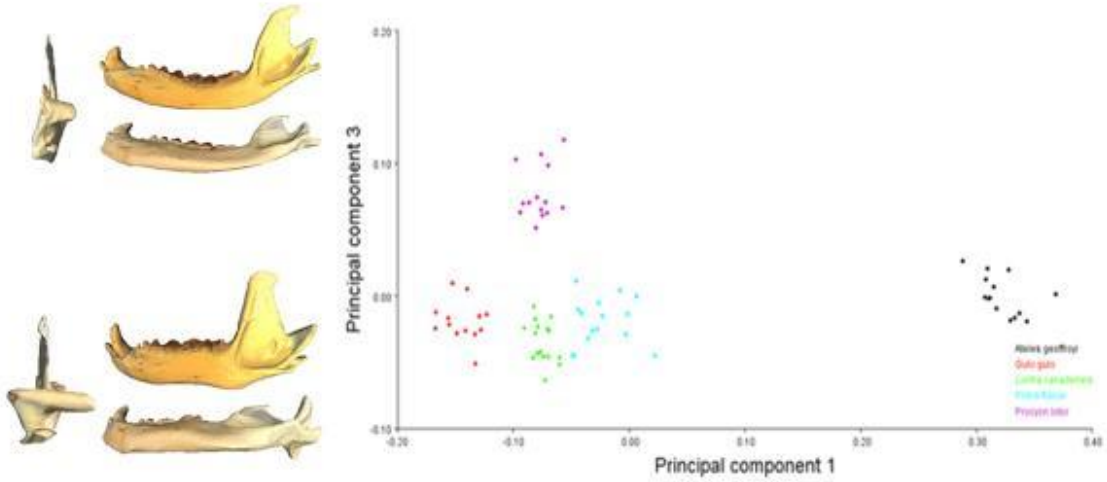

Figure 8. Results of the principal component analysis performed on Musteloidea mandibles with *Ateles geoffroyi*. Each dot represents a single specimen. Species are grouped by diet on PC3. Mandible views include lateral, latero-inferior, and caudal views.

Table 9. Independent contrasts values indicating no significant values in Musteloidea Mandible, Musteloidea with *Ateles* Mandible, Musteloidea with *Ateles* Cranium, and Musteloidea with *Ateles* and *Sarcophilus* Cranium analyses, meaning no further analysis is needed. The Musteloidea Cranium analysis indicates a significant difference, and further analysis is needed, found in Figures 10 & 11.

Independent Contrasts	
Data Set	p-value
Musteloidea Mandible	0.3320
Musteloidea with *Ateles* Mandible	0.6804
Musteloidea Cranium	<0.0001
Musteloidea with *Ateles* Cranium	0.4923
Musteloidea with *Ateles* and *Sarcophilus* Cranium	0.2293

I do find that some regression values are significant; however, due to the small percentage of pooled regression values (less than 2.5%). In relation to those p-values, I chose not

to remove size as it had very little effect on the results. A full table of results of the regression tests can be seen in Table 10.

Table 10. In both pooled and unpooled regression values, the data indicate no significant values within Musteloidea Cranium, Musteloidea with *Ateles* Cranium, and Musteloidea with *Ateles* and *Sarcophilus* Cranium analyses. The Musteloidea Mandible, and Musteloidea with *Ateles* Mandible indicates a significant difference within both the pooled and unpooled regression values.

Regression				
	Pooled		Unpooled	
	P-value	%	P-value	%
Musteloidea Mandible	<0.0001	1.8497	<0.0001	15.2611
Musteloidea With *Ateles* Mandible	<0.0001	2.2828	<0.0001	13.4846
Musteloidea Cranium	0.0008	4.9358	0.3180	2.0043
Musteloidea with *Ateles* Cranium	0.0448	2.3880	0.0671	3.4791
Musteloidea with *Ateles* and *Sarcophilus* Cranium	0.1357	1.6412	0.0344	3.5783

A PCA of the Musteloidea with *Ateles geoffroyi* articular surface can be seen in Figure 9, and PC information is provided in Table 8. The patterning and results highly resemble that of Figure 6. On the first PC axis, there is a distinct pattern to the data with strict carnivores at the negative end, and the strict herbivore to the positive end. PC1 (Figure 9) accounts for 53.7% of the variability in the sample and represents shape variation relating to the curvature of the mandibular condyle. Individuals at the negative end of PC1 (*Lontra canadensis*) have a very pronounced anteroposterior curvature to the mandibular condyle, while individuals at the positive end of PC1 (*Ateles geoffroyi*) have a considerably less curved mandibular condyle. On the second PC axis, like in the Musteloidea-only articular surface results, there is no distinct pattern. PC2 (Figure 9) accounts for 15.7% of the variability in the sample and represents shape variation relating to anterior-posterior curvature of the mandibular condyle. Individuals at the negative end of PC2 (*Ateles geoffroyi, Gulo gulo*) have a straight anterior edge of the condyle. Individuals near the positive end of PC2 (*Procyon lotor*) have a slightly curvature, or bowing,

with the middle of the condyle more posteriorly positioned. While there are differences in positive PC2 and negative PC2, the differences are much less dramatic than the results of PC1.

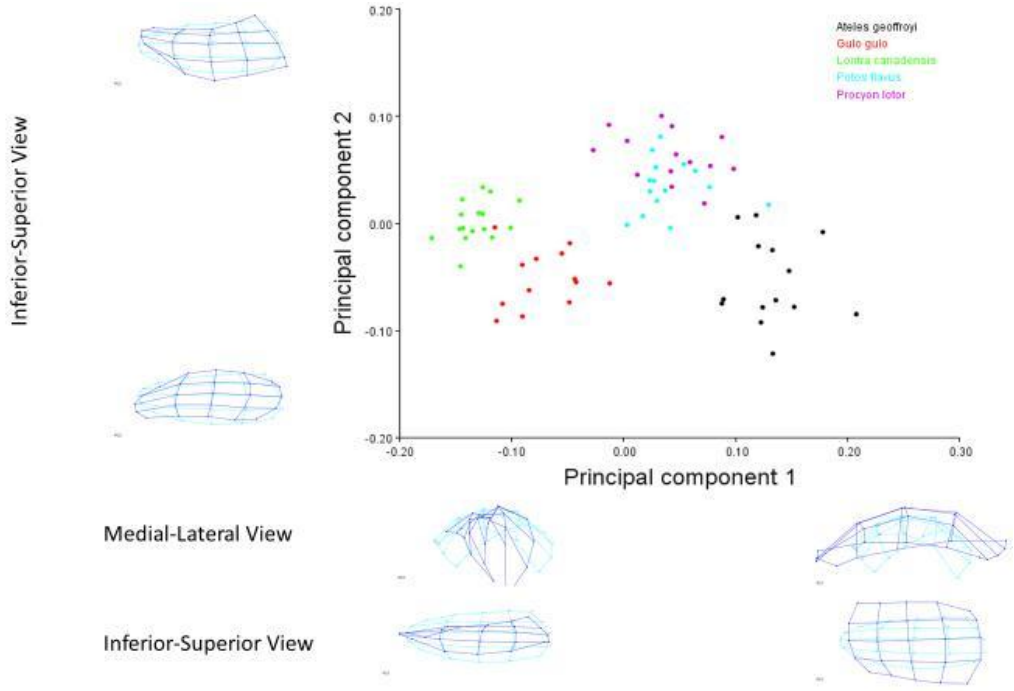

Figure 9. Results of the principal component analysis performed on Musteloidea with *Ateles geoffroyi* mandibular condyle. Each dot represents a single specimen. Species are grouped by diet on PC1. On PC1 axis, mandibular condyles are in medial-lateral view (top), inferior-superior view (bottom). There is no distinct patterning on PC2. The light blue represents the average with the PC change overlaid in a purple.

Crania

The PCA of the musteloid sample can be seen in Figures 10-11 and Table 8. On the first PC axis, there is a pattern to the data with herbivore and omnivore to the negative end and the carnivores to the positive. PC1 (Figure 10) accounts for 46.4% of the variability in the sample and represents shape variation in the mandibular fossa shape and curvature and the molar row length. Individuals at the negative end of PC1 (*Procyon lotor* and *Potos flavus*) display a broad curvature of the mandibular fossa, an articular surface that is narrower mediolaterally, and a long molar row. Individuals at the positive end of PC1 (*Lontra canadensis*) display tighter curvature

of the mandibular fossa along with a mediolaterally broader articular surface and a short molar row. On the second PC axis, the data pattern has omnivorous species to the positive end of the axis and the herbivorous and carnivorous to the negative end. PC2 (Figure 10) accounts for 26.7% of the variability in the sample and represents variation in snout length. Individuals at the negative end of PC2 (*Gulo gulo* and *Potos flavus*) display a short snout compared to the individuals at the positive end of PC2 *(Procyon lotor*) that display a longer snout. Lastly, on the third PC axis, there is no definitive pattern to the data, with all feeding types mixed throughout the graph. PC3 (Figure 11) containing 14.4% of the variation represents differences within the tooth row. Individuals at the negative end of PC3 (*Gulo gulo*) have a mediolateral curvature to the tooth row, whereas the individuals at the positive end of PC3 (*Potos flavus*) have a very straight, linear, tooth row. There is phylogenetic signal present within the sample group (Table 9) and the results are available in Figure 13 and Figure 14.

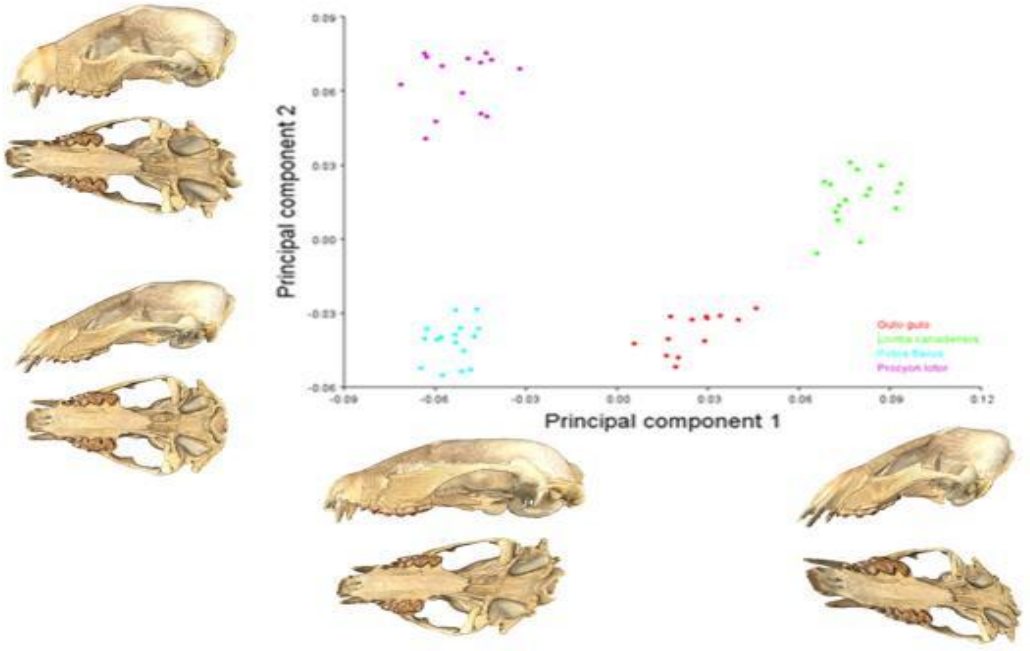

Figure 10. Results of the principal component analysis performed on Musteloidea crania. Each dot represents a single specimen. Species are grouped by diet on both PC1 and PC2. Cranial views include lateral (top) and inferior views (bottom).

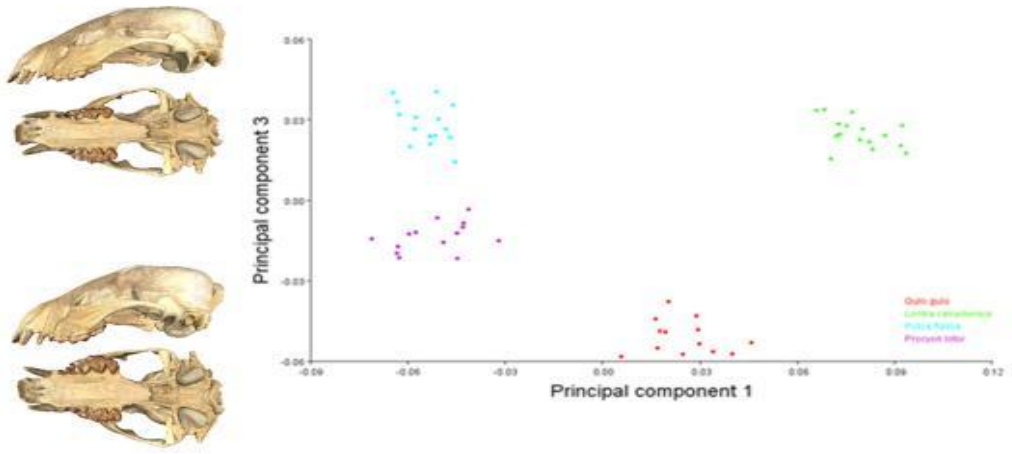

Figure 11. Results of the principal component analysis performed on Musteloidea crania. Each dot represents a single specimen. Species are grouped by palate shape on PC3. Cranial views include lateral and inferior views.

A PCA of the Musteloidea cranial articular surface can be seen in Figure 12, and PC information is provided in Table 8. The patterning and results resembles that of Figure 6. On the first PC axis, there is a distinct pattern to the data with strict carnivores at the positive end, and the strict herbivore to the negative end. PC1 (Figure 12) accounts for 61.9% of the variability in the sample and represents shape variation relating to the curvature of the mandibular fossa. Individuals at the positive end of PC1 (*Lontra canadensis*) have a very pronounced anteroposterior curvature to the mandibular fossa, while individuals at the negative end of PC1 (*Potos flavus*) have a considerably less curved mandibular fossa. On the second PC axis there is a pattern of strict herbivore and carnivore to the positive end, and omnivores to the negative, though there is slight overlap. PC2 (Figure 9) accounts for 11.0% of the variability in the sample

and represents shape variation relating medial-lateral orientation of the mandibular fossa. Individuals at the negative end of PC2 (*Procyon lotor*) have an angled mandibular fossa where the anterior portion is more medial, and the posterior portion is more lateral. Individuals near the positive end of PC2 (*Gulo gulo, Potos flavus*) have a more squared mandibular fossa, with the medial edge nearly parallel with the presumed midline of the skull.

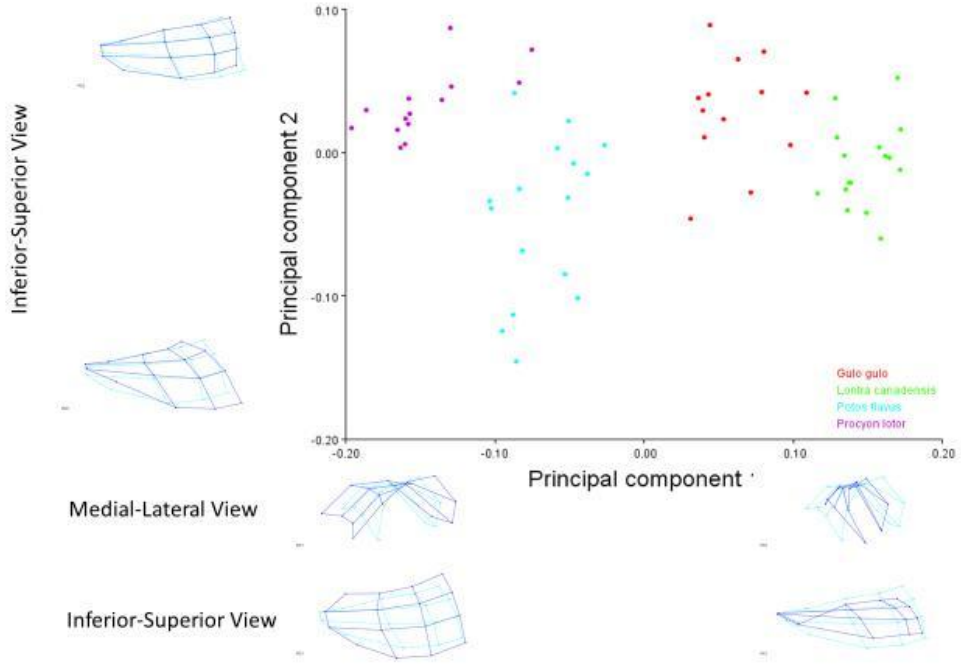

Figure 12. Results of the principal component analysis performed on Musteloidea mandibular fossa. Each dot represents a single specimen. Species are grouped by diet on PC1. On PC1 axis, the mandibular fossa are in medial-lateral view (top), inferior-superior view (bottom). There is some evidence suggesting strict carnivore/herbivore diet to the positive end and omnivore diet to the negative of PC2. The light blue represents the average with the PC change overlaid in a purple.

A phylogenetic PCA of the musteloid sample can be seen in Figures 13-14 and Table 8. On the first PC axis, there is a pattern to the data with the activity patterns of the species. PC1 (Figure 13) accounts for 46.5% of the variability within the sample and represents shape changes in the snout superior-inferior angulation, the distance between the maxillary tubercle (S4), and the most inferior point of the pterygoid plate (S5). Individuals at the positive end of PC1 (*Lontra*

canadensis) have a snout with no superior-inferior angulation and a short S4-S5 (maxillary tubercle-most inferior point of pterygoid plate) distance, whereas individuals at the negative end (*Potos flavus*) have a snout with a relatively high angulation and large S4-S5 (maxillary tubercle-most inferior point of pterygoid plate) distance. On the second PC axis, the data pattern has omnivorous species to the positive end of the axis and the herbivorous and carnivorous towards the negative end. PC2 (Figure 13) accounts for 34.8% of the variation and represents shape changes in the mandibular fossa and snout length. Individuals at the negative end of PC2 (*Lontra canadensis*) have an increased width in the mandibular fossa and a short snout. Individuals at the positive end of PC2 (*Procyon lotor*) have a much narrower fossa and longer snout. Lastly, the third PC axis exhibits a pattern to the data in a way that the herbivore and omnivore are to the negative end and the carnivores to the positive. PC3 (Figure 14) accounts for 18.8% of the shape variability pertaining to the curvature of the mandibular fossa and landmarks S3 (alveolar margin, midline M2) and S4 (maxillary tubercle) of the tooth rows. Individuals at the negative end of the spectrum (*Potos flavus*) have a much flatter mandibular fossa. Landmarks S3 (alveolar margin, midline M2) and S4 (maxillary tubercle) are more medially and no curvature to the tooth row was present. Individuals at the positive end of the spectrum (*Gulo gulo*) have a mandibular fossa with a much tighter curvature, and landmarks S3 (alveolar margin, midline M2) and S4 (maxillary tubercle) are more lateral, creating a wider and shorter palate. Thus, the individuals near the negative ends of PC3 have an overall appearance of a straight tooth row, whereas individuals at the positive end of PC3 have a mediolaterally arching tooth row.

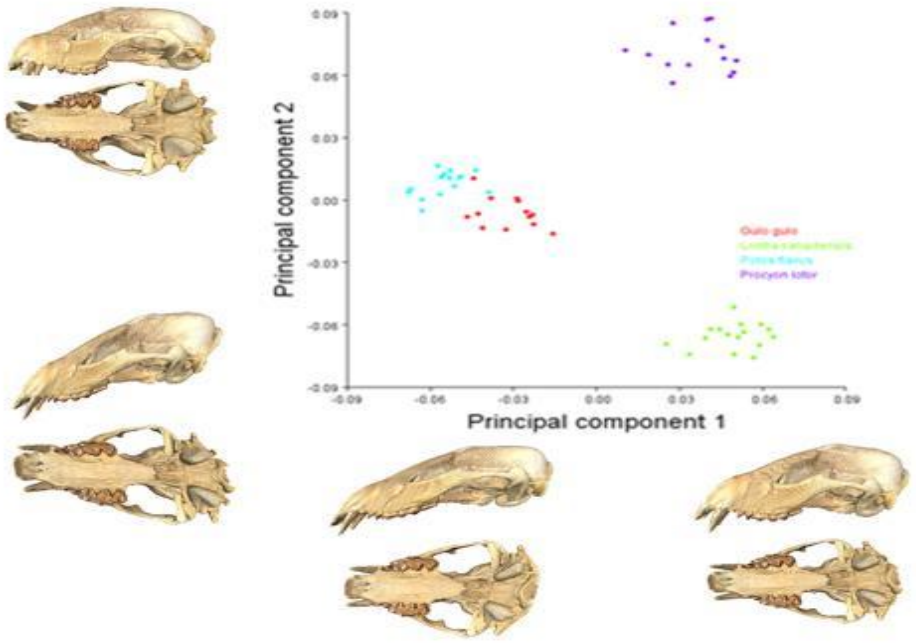

Figure 13 Results of the principal component analysis performed on the phylogenetically corrected Musteloidea crania. Each dot represents a single specimen. Species are grouped by muscle dependency on PC1 and diet on PC2. Cranial views include lateral and inferior views.

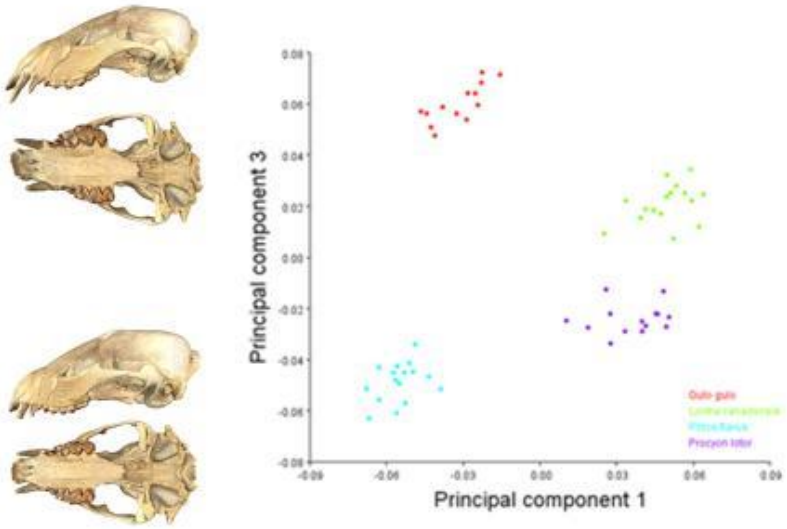

Figure 14. Results of the principal component analysis performed on the phylogenetically corrected Musteloidea crania. Each dot represents a single specimen. Species are grouped by diet on PC3. Cranial views include lateral and inferior views.

The Musteloidea crania with *Ateles* and *Sarcophilus* PCA's can be seen in Figures 15 -16 and Table 8. On the first PC axis, there is somewhat of an unexpected pattern to the data, that being *Sarcophilus harrisii*. Without *Sarcophilus* harrisii, PC1 exhibits the expected pattern with herbivorous species to the negative end, carnivorous to the positive end, and the omnivorous between. However, *Sarcophilus harrisii*, a strict carnivore, plots near the herbivorous species. PC1 (Figure 15) accounts for 57.6% of the shape variability relating to length of the cranium and mandibular fossa characteristics. Individuals at the negative end of PC1 (*Ateles geoffroyi)* display a longer cranium and a narrow, flat mandibular fossa. Individuals at the positive end of PC1 (*Lontra canadensis*) have a shorter cranium with a wide, tightly curved mandibular fossa.

On the second PC axis, there is no definitive pattern to the data, with all feeding types mixed throughout the graph. PC2 (Figure 15) accounts for 18.3% of the variability relating to shapes changes in the width of the cranium. Individuals at the negative end of PC2 (*Ateles geoffroyi*) exhibit a short mediolateral distance between landmarks S0 (alveolar margin, midline of skull) and S5 (most inferior point on pterygoid plate) and are nearly parallel to the midline of the skull. Individuals at the positive end of PC2 (*Sarcophilus harrisii*) exhibit a wider cranium, as the mediolateral distance between the same points are greater than those at the negative end. Lastly, along the third PC axis, a familiar pattern is exhibited with the carnivores and herbivores grouped tightly together on the negative end, and omnivores are the outlying group on the positive end. PC3 (Figure 16) accounts for 9.6% of the shape variation and relates to the snout length of the specimens. Individuals at the negative end of PC3 (*Procyon lotor*) display a long snout, whereas individuals at the positive end of PC3 (*Gulo gulo*) present much shorter snout length. There is no significant phylogenetic signal (Table 9), and the regression values also indicate no significance (Table 10).

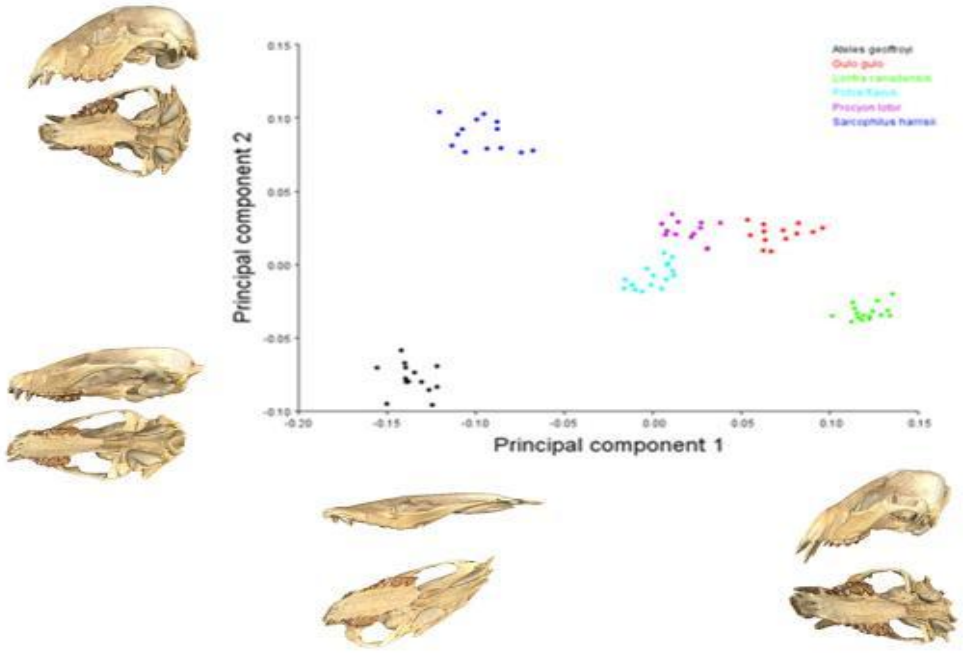

Figure 15. Results of the principal component analysis performed on the Musteloidea with *Ateles geoffroyi* and *Sarcophilus harrisii* crania. Each dot represents a single specimen. Species are grouped by diet on PC1 and palate shape on PC2. Cranial views include lateral and inferior views.

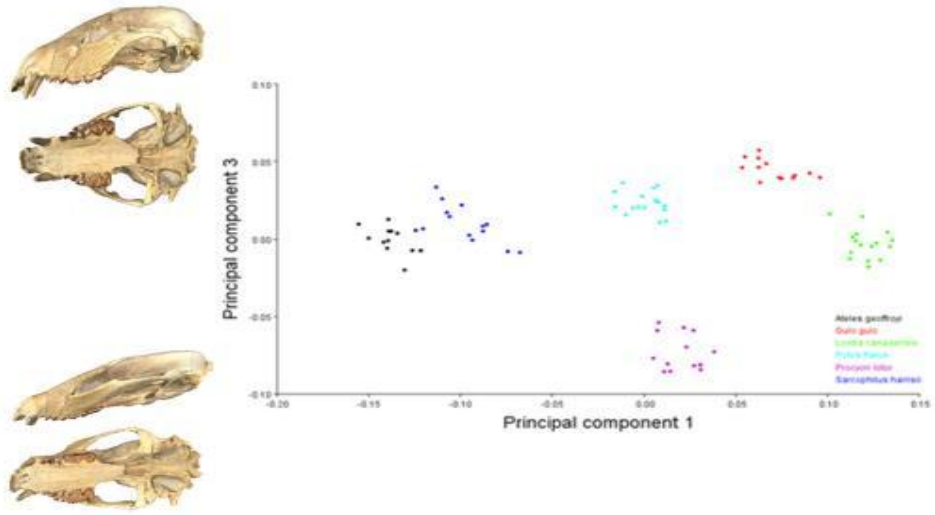

Figure 16. Results of the principal component analysis performed on the Musteloidea with *Ateles geoffroyi* and *Sarcophilus harrisii* crania. Each dot represents a single specimen. Species are grouped by diet on PC3. Cranial views include lateral and inferior views.

A PCA of the musteloids with *Ateles* geoffroyi and *Sarcophilus harrisii* cranial articular surface can be seen in Figure 17, and PC information is provided in Table 8. On the first PC axis, there is a distinct pattern to the data with strict carnivores at the positive end, and the strict herbivore to the negative end, though there is one exception, *Sarcophilus harrisii*. PC1 (Figure 17) accounts for 68.4% of the variability in the sample and represents shape variation relating to the curvature of the mandibular fossa. Individuals at the negative end of PC1 (*Lontra canadensis*) have a very pronounced anteroposterior curvature to the mandibular fossa, while individuals at the positive end of PC1 (*Ateles geoffroyi*) have a flat mandibular fossa. On the second PC there is a distinct patter with *Sarcophilus harrisii* offset from the other mammalian species. PC2 (Figure 17) accounts for 15.3% of the variability in the sample and represents shape

variation relating to anterior-posterior curvature of the mandibular fossa. Individuals at the positive end of PC2 (*Ateles geoffroyi, Gulo gulo, Lontra canadensis, Potos flavus, Procyon lotor*) have a fairly straight anterior and posterior edge to the condyle. The medial edge appears to have a superior-inferior curvature. Individuals near the negative end of PC2 (*Sarcophilus harrisii*) have an oval shaped mandibular fossa where the posterior edge is straight, and the anterior portion is curved, with the middle portion bowed anteriorly.

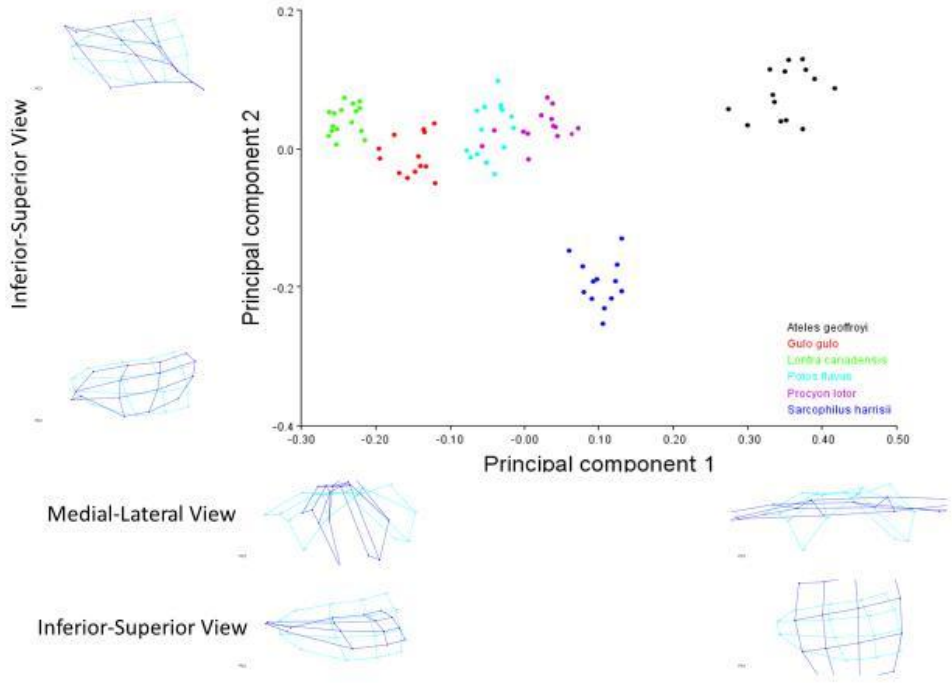

Figure 17. Results of the principal component analysis performed on Musteloidea mandibular fossa. Each dot represents a single specimen. Species are grouped by diet, with the exception of *Sarcophilus harrisii,* on PC1. On PC1 axis, the mandibular fossa are in medial-lateral view (top), inferior-superior view (bottom). Infraorder Marsupialia specie, *Sarcophilus harrisii,* to the negative end and all other mammalian species to the positive end of PC2. The light blue represents the average with the PC change overlaid in a purple.

Discussion

The hypothesis of the study was supported through the collected data. It was predicted that when there is a large percentage of meat in the diet of a musteloid, the mandibular fossa will have a more concave shape, a curvature matching convex mandibular condyle, shallower masseteric fossa, and increased in-lever out-lever distance. There are questions relating to *Sarcophilus harrisii* TMJ morphology and marsupial TMJ morphology more generally. It is found, however, that TMJ morphology is not solely responsible for the feeding type-diet relationship and other aspects, such as snout and mandible length, also show great shape variation. This relates morphology by feeding type, but also by many other factors including, but not limiting to, locomotor habitat and defense mechanisms such as jaw gape. The greatest piece of data leading to this conclusion is the need for phylogenetic correction in only the crania. Dumont *et al*. (2016) states that cranium shape is first a result of locomotor habitat, and second feeding type. The phylogenetic correction of the crania falls in this study exemplifies Dumont's findings. The results of this study show that the cranium is likely influenced by many selective pressures. For example, orbit size and orientation are directly related to activity pattern, diet, and locomotor habitat, (Cox, 2008; Dumont *et al*., 2016). Another example of a cranial feature includes the occipital condyles. In aquatic Mustelids, the occipital condyles are located more caudo-dorsally than its arboreal and terrestrial relatives, presumably for streamline swimming. Characteristics of the cranium not directly related to the feeding mechanism are also affected by diet. This is seen in braincase shape where herbivorous species have a rounder braincase in compared to omnivorous and carnivorous species (Dumont *et al*., 2016). This is true within this study as well because the cranial data did not clearly pattern to that of diet. In this study palate shape as shown in Figure 11 is an indicator. The musteloid species are mixed in the data set without a clear and distinct patter related to feeding type. As there was no phylogenetic signaling

in the mandibles of the Musteloidea, it's concluded that diet may be the only influence behind mandible shape. This is concluded as the landmarking protocol includes many morphologically influential points and the variation is consistent with feeding. These variations were related to diet consistently through each grouping including differences in the coronoid process, mandibular condyle, masseteric fossa, and mandible length.

Mandibles

Of the two skull components, it was more difficult to explain the variation in shape patterning in the mandible among the sampled species. The shape of the mandible was likely influenced by a multitude of factors including muscle dependency, diet, and a "reactionary" design based on cranial shape, though exclusively related to diet.

PC1 of the Musteloidea and PC2 of the Musteloidea and *Ateles geoffroyi* graphs displayed the same patterning of musteloid taxa and the same aspects of shape variation, most notably the angulation of the coronoid process and the angulation of the mandibular condyle inferiorly on the medial side. This is possibly due to the mechanical advantage of the morphology. As in-lever distance S5-P2-2 (most superior point of coronoid process to anterior mid-point of mandibular condyle) increases relative to out-lever distance S0-P2-2 (alveolar margin, midline I1 to anterior mid-point of mandibular condyle) mechanical advantage increases (Gittleman & Valkenburgh, 1997). These points are relative specific to the temporalis mechanical advantage (La Croix *et al.*, 2011). These graphs are as expected, as the increase of the meat in a mustelids diet, the more dependency on the temporalis mechanical advantage is expected. It is also important to note that *Ateles geoffroyi* on the PC2 axis Musteloidea and

Ateles geoffroyi graphs appears misplaced, however the angulation of the coronoid process is overshadowing the driving in-lever-out-lever relative distances.

Like the previous grouping, PC2 of the Musteloidea (Figure 5) and PC1 of the Musteloidea and *Ateles geoffroyi* (Figure 8) graphs displayed the same patterning of taxa and the same physical characteristics, the width of the masseteric fossae. The grouping of these species with *Lontra canadensis*, a carnivore, grouped with the herbivore and omnivore at first glance is a bit curious. With the masseteric fossae being the most notable change in both data sets, the reliance of the masseter muscle is of question. As stated previously, herbivores generally do not need to generate bite forces at larger gapes, but rather smaller gapes, and have a reliance on the masseter muscle. Thus, the masseter muscle tends to become more developed in herbivorous taxa (Dumont *et al.*, 2016). As mentioned previously, herbivorous mustelids have a simple digestive tract without a caecum, digestive microbiota with a low digestibility rate of cellulose and carbohydrates, and the inability to grind food. This requires for herbivorous carnivorans to consume large quantities of food, thus the development of large masseter and temporalis muscles (Figueirido, *et al.*, 2010). This is reinforced with the grouping of *Potos flavus*, *Procyon lotor*, and *Ateles geoffroyi*, as they all consume some plant matter. However, *Lontra canadensis* also grouped with these species, and while *Lontra canadensis* does rely heavily on the temporalis muscle, like other carnivores, it possesses hypertrophied jaw muscles compared to terrestrial animals (e.g., *Gulo gulo*), which is thought to allow the rapid jaw motion necessary for catching elusive fish with their mouths underwater (Timm-Davis *et al.*, 2015). All these similarities are based on feeding, though the morphological similarities may be coincidental based on differing functions.

Lastly for the overall shape of the mandible, PC3 of both the Musteloidea (Figure 5) and Musteloidea with *Ateles geoffroyi* (Figure 7) presented the same characteristic, as mandible length was the overwhelmingly obvious difference between the two groupings. The herbivorous and carnivorous species were grouped together, and the outlying group was that of the omnivore. This is as expected as Dumont *et al.* (2016) states that herbivorous and carnivorous species have shorter snouts, whereas the snout is longer in the omnivorous species. This relationship will be later discussed with the cranium patterns as the mandible length is directly related to snout length.

The most relevant observations to this study is the shaping of the articulating surfaces. The articulating surface of the mandible, the mandibular condyle, exhibited morphology as expected. The carnivorous species, *Lontra canadensis* and *Gulo gulo*, were grouped overlapping each other on PC1 of both the Musteloidea mandible articulating surface (Figure 6) and Musteloidea with *Ateles geoffroyi* mandible articulating surface (Figure 9). The herbivorous and omnivorous species, *Potos flavus* and *Procyon lotor* occupied the same portion of the graph in PC1 of both the Musteloidea mandible articulating surface (Figure 6) and Musteloidea with *Ateles geoffroyi* mandible articulating surface (Figure 9). When *Ateles geoffroyi* was added to the mix, it occupied the same regions as *Potos flavus* and *Procyon Lotor* of PC1 in the graph, Musteloidea with *Ateles geoffroyi* (Figure 9). One thing should be noted is that there are no distinct groupings separating *Potos flavus* and *Procyon Lotor,* possibly suggesting that herbivorous carnivorans are morphologically restricted.

PC2 in both the Musteloidea mandible articulating surface (Figure 6) and Musteloidea with *Ateles geoffroyi* mandible articulating surface (Figure 9) both saw morphological differences. However, there is little to makes special notes about as PC1 accounted for >50%

variation in both instances and proved the prediction table regarding mandibular condyle convexity, snout length, and masseteric fossa shape.

Crania

The crania showed much clearer patterning than the mandible, although the same characteristics including diet, snout length, and palate were exhibited throughout the data. PC1 of the Musteloidea analysis, PC3 of the phylogenetically corrected Musteloidea analysis, and PC1 of the Musteloidea with *Ateles geoffroyi* and *Sarcophilus harrisii* analysis displayed the same patterning among species and the same physical characteristics with one exception, *Sarcophilus harrisii*. The overwhelming trait that was exemplified in these PCs was the shape of the mandibular fossa. Generally, as expected, the carnivorous species had a more concave mandibular fossa than the herbivorous and omnivorous species. Because PC1 of the Musteloidea analysis and PC3 of the phylogenetically corrected Musteloidea analysis both had shape changes to the mandibular fossa, it would suggest that the morphology of the mandibular fossa is limited by phylogeny. Once phylogeny is accounted for, the mandibular fossa is no longer the morphological characteristic most greatly influenced by diet as shown in the PC results of the corrected and non-corrected data. The one exception is *Sarcophilus harrisii*, who was closer to the herbivorous *Ateles geoffroyi*, and exhibited a flatter fossa with little restriction to the TMJ. This may be due to the need for jaw gape. *Ateles geoffroyi* has an average jaw gape of 78.1 degrees (Wall, 1999), *Procyon lotor* has a jaw gape of 54.8 degrees, and *Gulo gulo* has a jaw gape of 44.2 degrees (Christiansen & Adolfssen, 2005). *Potos flavus* and *Lontra canadensis* jaw gapes are unknown but are expected to be similar to their sister taxa, *Procyon lotor* and *Gulo gulo*, respectively. *Sarcophilus harrisii* was the unexpected group where jaw gape can be seen at an expected angle between 75 and 80 degrees (Attard *et al*, 2011). This suggests that mandibular

fossa morphology may be influenced by other factors other than feeding type alone, with some evidence pointing towards vocalization or a threat display (Attard *et al.*, 2011).

PC2 of the Musteloidea analysis, PC2 of the phylogenetically corrected Musteloidea analysis, and PC3 of the Musteloidea with *Ateles geoffroyi* and *Sarcophilus harrisii* analysis displayed the same patterning of taxa and the same physical characteristic of snout length. It is well-documented that snout length is related to feeding as herbivores and carnivores have shorter snouts and omnivores the longer snouts. Snout length correlates with the jaw outlever and thus a short snout increases the mechanical advantage for biting, as it increases the bite force (Dumont *et al.*, 2016). This was shown by Christiansen and Wroe (2007). These authors studied bite forces (BF) and corrected for body mass in a bite force quotient (BFQ), allowing researchers to study bite forces across species with different body sizes. Two different measures of BFQ were measured in newtons (N), BFQ at the canine (BFQ_{ca}) and the carnassials (BFQ_{carn}). The short snout musteloids of this sample include the herbivorous *Potos flavus* (BFQ_{ca}: 123.8; BFQ_{carn}: 101.7) and the carnivorous species *Gulo gulo* (BFQ_{ca}: 104.6; BFQ_{carn}: 106.2) and *Lontra canadensis* (BFQ_{ca}: 101.9; BFQ_{carn}: 100.3). The long-snouted omnivorous *Procyon lotor* (BFQ_{ca}: 78.2; BFQ_{carn}: 73.7) shows a huge drop-off in newtons generated (Christiansen and Wroe, 2007). It is believed that *Potos flavus* has such large BFQ_{ca} as an adaptation for tearing into fruit, as its BFQ_{carn} is average for a carnivore (Christiansen and Wroe, 2007). Based on Figures 10, 13, and 16, we expect the BFQ of *Ateles geoffroyi* and *Sarcophilus harrisii* to generate around the same numbers based on snout length. There have been several studies where length of the snout has been correlated with bite force across several clades (Aguirre *et al.*, 2002, 2003; Figueirido *et al.*, 2010, 2011a, 2011b; Herrel *et al.*, 2007; Herrel, De Grauw & Lemos-Espinal, 2001; Kohlsdorf *et al.*, 2008; Marshall *et al.*, 2012; Santana, Dumont & Davis, 2010; Verwaijen, Van Damme, &

Herrel, 2002;). Although herbivorous musteloids have shortened snouts, they maintain a long tooth row as they need to increase their bite force but also maintain a large occlusal area, shifting the palate posteriorly (Christiansen and Wroe, 2007). With the increased length of the snout, the omnivorous Musteloidea sacrifice bite force. This is shown in the following PCs in their relation to palate.

PC3 of the Musteloidea analysis and PC2 of the Musteloidea with *Ateles geoffroyi* and *Sarcophilus harrisii* graphs displayed the same patterning and the same physical characteristics, shape of the palate and tooth row. The positive end of PC3 of the Musteloidea, and the negative end PC2 of the Musteloidea with *Ateles geoffroyi* and *Sarcophilus harrisii* have the widest point of the palate as S1 (alveolar margin, midline canine). However, the negative end of PC3 of the Musteloidea, and the positive end PC2 of the Musteloidea with *Ateles geoffroyi* and *Sarcophilus harrisii* have the widest point of the palate at S3 (alveolar margin, midline M2). Shortening the width of the palate is a characteristic of animals that consume hard prey (Timm-Davis *et al.*, 2015). This may be a piece of the answer to the width of the palate; however, it does leave some questions as *Lontra canadensis*, a mollusk and shell crusher, is opposite the bone-crushing *Sarcophilus harrisii* and could make for an interesting future study. One explanation to this statistical display could be size of the prey. In canids, species with short, broad muzzles, larger incisors and canines, and relatively large carnassials are consistent with higher bite forces and thus ability to kill prey larger than themselves (Meloro *et al.*, 2015).

PC1 of the phylogenetically corrected Musteloidea displays a patterning in which the distance between S4 (maxillary tubercle) and S5 (most inferior point on pterygoid plate) increases towards the negative end. The medial pterygoid originates at the lateral pterygoid plate of the sphenoid, with few fibers originating from the maxillary tubercle, and attaches at the

bottom of the ascending ramus to the posterior edge of the angular process (Alomar *et al.*, 2007; Christiansen & Adolfssen, 2005; Davis, 2014). Being that *Gulo gulo* and *Potos flavus* are grouped together, and *Lontra canadensis* and *Procyon lotor* are grouped together, there is evidence to suggest that the dependency on the medial pterygoid is not related to feeding ecology directly or it could be a function of bite force as *Gulo gulo* and *Potos flavus* both have larger BFQ_{ca} and BFQ_{carn} values than *Lontra canadensis* and *Procyon lotor*.

The most relevant aspect of the cranium to this study is the shaping of the articulating surface. The articulating surface of the cranium, the mandibular fossa, exhibited morphology as expected, like the articulating surface of the mandible. The carnivorous species, *Lontra canadensis* and *Gulo gulo*, were grouped next to each other on PC1 of both the Musteloidea cranium articulating surface (Figure 12) and Musteloidea with *Ateles geoffroyi* and *Sarcophilus harrisii* cranium articulating surface (Figure 17). The herbivorous and omnivorous species, *Potos flavus* and *Procyon lotor* occupied overlapping portions of the graph other on PC1 of both the Musteloidea cranium articulating surface (Figure 12) and Musteloidea with *Ateles geoffroyi* and *Sarcophilus harrisii* cranium articulating surface (Figure 17). When *Ateles geoffroyi* and *Sarcophilus harrisii* were added to the sample, they occupied the regions more positive as *Potos flavus* and *Procyon Lotor* of PC1 on the graph, Musteloidea with *Ateles geoffroyi* and *Sarcophilus harrisii* cranium articulating surface (Figure 17). While there is no overlap between *Ateles geoffroyi* and any other species, *Sarcophilus harrisii* has some overlap with *Procyon lotor*. There is some curious positionings to the species on Musteloidea with *Ateles geoffroyi* and *Sarcophilus harrisii* cranium articulating surface (Figure 17) as *Procyon lotor* and *Sarcophilus harrisii*, an omnivore and carnivore respectively, occupy regions more positive than *Potos flavus*.

Limitations and Future Avenues

There were some limitations to this study that would be able to be remedied in future studies using this landmark protocol. The first limitation would be the specimen collection for *Sarcophilus harrisii*. Unfortunately, only cranial specimens were able to be collected in preparation for this project as the mandible specimens were unavailable. For a better, more accurate study, the inclusion of the *Sarcophilus harrisii* mandible would influence the data and could potentially change the interpreted statistical outcomes. In addition to the lack of mandible data collection for *Sarcophilus harrisii*, sex data was unavailable for it and *Lontra canadensis*. Ultimately, I believe it had little effect on the overall outcome of this study because with the sample sizes of *Sarcophilus harrisii* (13) and *Lontra canadensis* (16) and there was no separation of sexes in the other species.

The largest limitation to this study was the selection of species to be used as controls. I think the study could have been more conclusive if different controls were used in the study. *Sarcophilus harrisii* and *Ateles geoffroyi* may have been too far removed from Musteloidea for this study at 160.0 Ma (Cao *et al.*, 2000) and 83.8 Ma (dos Reis, 2012) respectively. It would have been advantageous to use species within Carnivora to use as controls. For example, a carnivorous feline such as *Lynx rufus* (McLean *et al.*, 2005) and herbivorous *Ailuropoda melanoleuca* (Wang, 2017) may provide for better controls as they're more closely related within order Carnivora.

Despite the limitations to this study, it opens the opportunity to further investigate morphology of the TMJ within Musteloidea. I am satisfied with the landmarking protocol of this study and moving forward would choose to use the same protocol. I would first implement more appropriate controls as already touched on. The second course of action would include adding

more species of Musteloidea including herbivores, omnivores, and carnivores. As mentioned, Musteloidea includes over 82 species (Dumont *et al.*, 2016) and including more species would give more data and potentially solidify the trends of shown in the data within this study. Once these two limitations are addressed, this would allow for research studies to work backwards through the phylogenetic tree. From there it could be determined if these assumptions are true in superfamily Musteloidea, infraorder Arctoidea, suborder Caniforma, order Carnivora, class Mammalia, and eventually across kingdom Animalia.

Overall Conclusions

Some of the hypotheses of the study were fully supported. I find that the curvature of the condylar head of the mandible and the mandibular fossa of the crania are related to feeding type. However, there are many aspects that influence the relationship of morphology and feeding type and more research is needed to fully conclude the overall relationship. This is exemplified by the descriptions of data above, relating the differing species by not only feeding type, but other factors such as jaw gape.

There were some unexpected results, however. *Sarcophilus harrisii* did not follow the expectations of a meat-eating species as seen in Figure 15, Figure 16, and Figure 17. *Sarcophilus harrisii* was expected to occupy the same regions of the graphs as the other carnivores, *Gulo gulo* and *Lontra canadensis*. This is particularly true of PC1 and PC3 in Figure 15 and Figure 16, and PC1 and PC2 of Figure 17 where the species can be seen occupying similar regions as *Ateles geoffroyi*. One explanation for this result is that the controls in the study are too far removed evolutionary speaking and controls more closely related to Musteloidea would result in a more expected result as environmental stresses would have a more consistent morphological impact on shape. Perhaps, the environmental stresses such as locomotor habitat, activity pattern, threat displays or even mating displays could influence morphology greater than feeding ecology alone though much more research is needed to make a distinct conclusion. Another unexpected result was the need for phylogenetic corrections in only the Musteloidea crania and not the mandible in the same grouping of species. I found this odd as the relatedness of the cranium and mandible, and only one needing a phylogenetic correction. This might suggest that the muscles of mastication may have a greater influence in mandible morphology than the cranium, which has many selective pressures.

Many shape morphologies are correlated with feeding. While the curvature of the mandibular fossa and condylar head have relation to the feeding types, its only part of the overall morphology relating to feeding type. The mandible had major axes of shape variation relating to the angle of the coronoid process, the width and depth of the masseteric fossa, placement and shape of the condylar head, the placement of the articular surface of the condylar head, and width and curvature of the condylar head. As Dumont *et al*. (2016) found, cranial shape is first a result of locomotor habitat, and second feeding type. While each of these characteristics are related to feeding, through this study, it is not clear as to whether they are related to locomotor habitat, feeding type, or some other evolutionary stress directly as other evolutionary environmental stresses were not controlled for (i.e., locomotor habitat.)

As seen with both the mandible and crania results, many shape morphologies are related to feeding in addition to the shape of the condyle and fossa. The cranium displayed changes related to feeding type including snout length, shape of the tooth rows, width of the fossa, as well as the predicted mandibular fossa curvature. The features of both the mandible and cranium follow the generalized assumptions of morphology within Musteloidea (snout length, palate width, condyle curvature, etc.) but is difficult to attribute these changes to feeding type alone. Overall, it would be interesting to further study Infraorder Marsupialia, including *Sarcophilus harrisii,* and investigate the differences in the TMJ morphology as *Sarcophilus harrisii*, doesn't seem to meet the generalized Carnivoran TMJ morphology assumptions.

Literature Cited

Adams, D. C., & Otárola-Castillo, E. (2013). geomorph: an R package for the collection and analysis of geometric morphometric shape data. *Methods in Ecology and Evolution*, *4*(4), 393-399.

Adams, D., Rohlf, F., & Slice, D. (2004). Geometric morphometrics: Ten years of progress following the 'revolution'. Italian Journal of Zoology, 71(1), 5-16.

Alomar, X., Medrano, J., Cabratosa, J., Clavero, J. A., Lorente, M., Serra, I., Salvador, A. (2007). Anatomy of the temporomandibular joint. Seminars in Ultrasound, CT, and MRI, 28(3), 170-183.

Aguirre, L. F., Herrel, A., Damme, R. v., & Matthysen, E. (2002). Ecomorphological analysis of trophic niche partitioning in a tropical savannah bat community. Proceedings of the Royal Society of London. Series B: Biological Sciences, 269(1497), 1271-1278.

Aguirre, L. F., Herrel, A., Damme, R. V., & Matthysen, E. (2003). The implications of food hardness for diet in bats. Functional Ecology, 17(2), 201-212.

Arnason, U., Gullberg, A., Janke, A., Kullberg, M., Biologiska institutionen, Molekylär cellbiologi. Faculty of Science. (2007). Mitogenomic analyses of caniform relationships. Molecular Phylogenetics and Evolution, 45(3), 863-874.

Arnold, C., L. J. Matthews, and C. L. Nunn. (2010). The 10kTrees Website: A New Online Resource for Primate Phylogeny. Evolutionary Anthropology 19:114-118.

Asahara, M., Saito, K., Kishida, T., Takahashi, K., & Bessho, K. (2016). Unique pattern of dietary adaptation in the dentition of carnivora: Its advantage and developmental origin. Proceedings of the Royal Society b-Biological Sciences, 283(1832)

Attard, M. R. G., Chamoli, U., Ferrara, T. L., Rogers, T. L., & Wroe, S. (2011). Skull mechanics and implications for feeding behaviour in a large marsupial carnivore guild: The thylacine, tasmanian devil and spotted-tailed quoll. Journal of Zoology, 285(4), 292-300.

Bookstein F. L., 1991 - Morphometric tools for landmark data: geometry and biology. Cambridge University Press, Cambridge.

Bourke, J., Wroe, S., Moreno, K., McHenry, C., & Clausen, P. (2008). Effects of gape and tooth position on bite force and skull stress in the dingo (canis lupus dingo) using a 3-dimensional finite element approach. PloS One, 3(5), e2200.

Bramble, D. M. (1978). Origin of the mammalian feeding complex; models and mechanisms. Paleobiology, 4(3), 271-301.

Cadima, Jorge F. C. L. & Jolliffe, I. T. (1996). Size- and shape-related principal component analysis. Biometrics, 52(2), 710-716.

Cao, Y., Fujiwara, M., Nikaido, M., Okada, N., & Hasegawa, M. (2000). Interordinal relationships and timescale of eutherian evolution as inferred from mitochondrial genome data. Gene, 259(1), 149-158.

Chapman, C. (1987). Flexibility in diets of three species of Costa Rican primates. Folia Primatologica, 49(2), 90-105.

Christiansen, P., & Adolfssen, J. S. (2005). Bite forces, canine strength and skull allometry in carnivores (mammalia, carnivora). Journal of Zoology, 266(2), 133-151.

Christiansen, P., & Wroe, S. (2007). Bite forces and evolutionary adaptations to feeding ecology in carnivores. Ecology, 88(2), 347-358.

Cooke, S. B., & Terhune, C. E. (2015). Form, function, and geometric morphometrics. The Anatomical Record, 298(1), 5-28.

Cox, P. G. (2008). A quantitative analysis of the Eutherian orbit: correlations with masticatory apparatus. Biological Reviews, 83(1), 35-69.

Davis, J. S. (2014). *Functional Morphology of Mastication in Musteloid Carnivorans* (Doctoral dissertation, Ohio University).

Druzinsky, R. E., Doherty, A. H., & De Vree, F. L. (2011). Mammalian masticatory muscles: Homology, nomenclature, and diversification. Integrative and Comparative Biology, 51(2), 224-234.

Dumont, M., Wall, C. E., Botton-Divet, L., Goswami, A., Peigné, S., & Fabre, A. (2016). Do functional demands associated with locomotor habitat, diet, and activity pattern drive skull shape evolution in musteloid carnivorans? Biological Journal of the Linnean Society, 117(4), 858-878.

Ercoli, M. D., Álvarez, A., Stefanini, M. I., Busker, F., & Morales, M. M. (2015). Muscular anatomy of the forelimbs of the lesser grison (galictis cuja), and a functional and phylogenetic overview of mustelidae and other caniformia. Journal of Mammalian Evolution, 22(1), 57-91.

Fabre, A. C., Goswami, A., Peigné, S., & Cornette, R. (2014). Morphological integration in the forelimb of musteloid carnivorans. *Journal of anatomy*,*225*(1), 19-30.

Fabre, A., Cornette, R., Peigné, S., & Goswami, A. (2013). Influence of body mass on the shape of forelimb in musteloid carnivorans. Biological Journal of the Linnean Society, 110(1), 91-103.

Figueirido, B., Serrano-Alarcón, F. J., Slater, G. J., & Palmqvist, P. (2010). Shape at the cross-roads: Homoplasy and history in the evolution of the carnivoran skull towards herbivory. Journal of Evolutionary Biology, 23(12), 2579-2594.

Figueirido, B., Palmqvist, P., Pérez-Claros, J. A., & Dong, W. (2011a). Cranial shape transformation in the evolution of the giant panda (ailuropoda melanoleuca). Naturwissenschaften, 98(2), 107-116.

Figueirido, B., MacLeod, N., Krieger, J., Renzi, M. D., Pérez-Claros, J. A., & Palmqvist, P. (2011b). Constraint and adaptation in the evolution of carnivoran skull shape. Paleobiology, 37(3), 490-518.

Gittleman, J. L., & Valkenburgh, B. V. (1997). Sexual dimorphism in the canines and skulls of carnivores: Effects of size, phylogency, and behavioural ecology. Journal of Zoology, 242(1), 97-117

Goswami, A. (2006). morphological integration in the carnivoran skull. Evolution, 60(1), 169-183.

Herrel, A., De Grauw, E., & Lemos-Espinal, J. A. (2001). Head shape and bite performance in xenosaurid lizards. Journal of Experimental Zoology, 290(2), 101-107.

Herrel, A., Schaerlaeken, V., Meyers, J. J., Metzger, K. A., & Ross, C. F. (2007). The evolution of cranial design and performance in squamates: Consequences of skull-bone reduction on feeding behavior. Integrative and Comparative Biology, 47(1), 107-117.

Herring, S.W. "TMJ Anatomy and Animal Models." *Journal of Musculoskeletal & Neuronal Interactions* 3, no. 4 (December 2003): 391.

Hylander, W. L. (2006). Functional anatomy and biomechanics of the masticatory apparatus. Temporomandibular disorders: an evidenced approach to diagnosis and treatment. New York: Quintessence Pub Co.

Inman, R. M., & Packila, M. L. (2015). Wolverine (gulo gulo) food habits in greater yellowstone. The American Midland Naturalist, 173(1), 156-161.

Kays, R. W. (1999). Food preferences of kinkajous (potos flavus): A frugivorous carnivore. Journal of Mammalogy, 80(2), 589-599.

Klingenberg, C. P. 2011. MorphoJ: an integrated software package for geometric morphometrics. *Molecular Ecology Resources* 11: 353-357.

Kohlsdorf, T., Grizante, M. B., Navas, C. A., & Herrel, A. (2008). Head shape evolution in tropidurinae lizards: Does locomotion constrain diet? Journal of Evolutionary Biology, 21(3), 781-790.

La Croix, S., Zelditch, M. L., Shivik, J. A., Lundrigan, B. L., & Holekamp, K. E. (2011). Ontogeny of feeding performance and biomechanics in coyotes. Journal of Zoology, 285(4), 301-315

Marshall, C. D., Guzman, A., Narazaki, T., Sato, K., Kane, E. A., & Sterba-Boatwright, B. D. (2012). The ontogenetic scaling of bite force and head size in loggerhead sea turtles (caretta caretta): Implications for durophagy in neritic, benthic habitats. The Journal of Experimental Biology, 215(Pt 23), 4166-4174.

Maynard Smith J, Savage RJG. (1959). The mechanics of mammalian jaws. School Sci Rev 141:289 301.

McLean, M. L., McCay, T. S., & Lovallo, M. J. (2005). Influence of age, sex and time of year on diet of the bobcat (lynx rufus) in pennsylvania. The American Midland Naturalist, 153(2), 450-453.

McMillan, B. R., Day, C. C., & Westover, M. D. (2015). Seasonal diet of the northern river otter (lontra canadensis): What drives prey selection? Canadian Journal of Zoology, 93(3), 197-205.

Meloro, C., Hudson, A., & Rook, L. (2015). Feeding habits of extant and fossil canids as determined by their skull geometry. Journal of Zoology, 295(3), 178-188.

Noble, H. W. (1973). Comparative functional anatomy of temporomandibular joint. Oral Sciences Reviews, 2, 3.

Pemberton, D., Gales, S., Bauer, B., Gales, R., Lazenby, B., & Medlock, K. (2008). The diet of the Tasmanian devil, Sarcophilus harrisii, as determined from analysis of scat and stomach contents. In Papers and Proceedings of the Royal Society of Tasmania (Vol. 142, No. 2, pp. 13-22).

Polly, P., Lawing, A., Fabre, A., & Goswami, A. (2013). Phylogenetic principal components analysis and geometric morphometrics. Hystrix-Italian Journal of Mammalogy, 24(1), 33-41.

Reis, M. d., Inoue, J., Hasegawa, M., Asher, R. J., Philip C. J. Donoghue, & Yang, Z. (2012). Phylogenomic datasets provide both precision and accuracy in estimating the timescale of placental mammal phylogeny. Proceedings: Biological Sciences, 279(1742), 3491-3500.

Revell, L. J. (2009). Size-correction and principal components for interspecific comparative studies. Evolution, 63(12), 3258-3268.

Ringnér, M., Onkologi, L., Faculty of Medicine, Department of Clinical Sciences, Lund, Lunds universitet, Medicin, Division V. (2008). What is principal component analysis? Nature Biotechnology, 26(3), 303-304.

Rulison, E.L., L. Luiselli, and R.L. Burke. "Relative Impacts of Habitat and Geography on Raccoon Diets." *The American Midland Naturalist* 168, no. 2 (October 2012): 231+.

Santana, S. E., Dumont, E. R., & Davis, J. L. (2010). Mechanics of bite force production and its relationship to diet in bats. Functional Ecology, 24(4), 776-784.

Santana, S.E. (2016), Quantifying the effect of gape and morphology on bite force: biomechanical modelling and *in vivo* measurements in bats. Funct Ecol, 30: 557-565.

Scapino, R. P. (1976). Function of the digastric muscle in carnivores. Journal of Morphology, 150(4), 843-859.

Slater, G. J., Harmon, L. J., & Alfaro, M. E. (2012). integrating fossils with molecular phylogenies improves inference of trait evolution. Evolution, 66(12), 3931-3944.

Sundberg, P. (1989). Shape and size-constrained principal components analysis. Systematic Zoology, 38(2), 166-168.

Terhune, C. E., Iriarte-Díaz, J., Taylor, A. B., & Ross, C. F. (2011). The instantaneous center of rotation of the mandible in nonhuman primates. Integrative and Comparative Biology, 51(2), 320-332.

Timm-Davis, L. L., DeWitt, T. J., & Marshall, C. D. (2015). Divergent skull morphology supports two trophic specializations in otters (lutrinae).

Turnbull, W. D. (1970). Mammalian masticatory apparatus. *Fieldiana Geology*, *18*, 147-356.

Valkenburgh, B. V. (2007). Déjà vu: The evolution of feeding morphologies in the carnivora. Integrative and Comparative Biology, 47(1), 147-163.

van Eijden, T. M. G. J., & Koolstra, J. H. (1998). A model for mylohyoid muscle mechanics. Journal of Biomechanics, 31(11), 1017-1024.

Verwaijen, D., Damme, R. V., & Herrel, A. (2002). Relationships between head size, bite force, prey handling efficiency and diet in two sympatric lacertid lizards. Functional Ecology, 16(6), 842-850.

Wall, C. E. (1999). A model of temporomandibular joint function in anthropoid primates based on condylar movements during mastication. American Journal of Physical Anthropology, 109(1), 67-88.

Wang, H., Zhong, H., Hou, R., Ayala, J., Liu, G., Yuan, S., Wu, D. (2017). A diet diverse in bamboo parts is important for giant panda (ailuropoda melanoleuca) metabolism and health. Scientific Reports, 7(1), 3377-13.

Wang, L., Lazebnik, M., & Detamore, M. S. (2009). Hyaline cartilage cells outperform mandibular condylar cartilage cells in a TMJ fibrocartilage tissue engineering application. Osteoarthritis and Cartilage, 17(3), 346-353.

Wang, Y., Liu, C., Rohr, J., Liu, H., He, F., Yu, J., Chen, Y. (2011). Tissue interaction is required for glenoid fossa development during temporomandibular joint formation. Developmental Dynamics, 240(11), 2466-2473.

Wiley, D.F., Amenta, N., Alcantara, D.A., Ghosh, D., Kil, Y.J., Delson, E., Harcourt-Smith, W.E.H., Rohlf, F.J., St. John, K., Hamann, B., 2005. Evolutionary morphing. Proc. IEEE Visualizations, 431-438.

Wroe, S., & Milne, N. (2007). convergence and remarkably consistent constraint in the evolution of carnivore skull shape. Evolution, 61(5), 1251-1260.

Yamaoka, M., Furusawa, K., Fujimoto, K., Iguchi, K., & Kumai, T. (1992). muscle-spindles in the mylohyoid muscle of rats. International Journal of Oral and Maxillofacial Surgery, 21(5), 309-31